in a 2D Square Domain : a Numerical and Experimental Approach

by

K. SARATH BABU

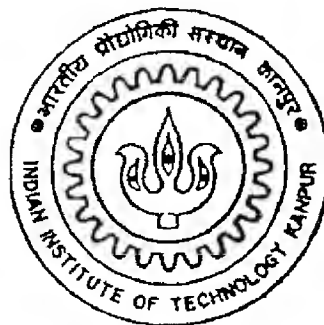DEPARTMENT OF MECHANICAL ENGINEERING

INDIAN INSTITUTE OF TECHNOLOGY KANPUR

FEBRUARY, 1999

On the Stability of a Numerical Algorithm for the Inverse Determination of Thermal conductivity in a 2D Square Domain : a Numerical and Experimental Approach

A thesis Submitted

in Partial Fulfilment of the Requirements

for the Degree of

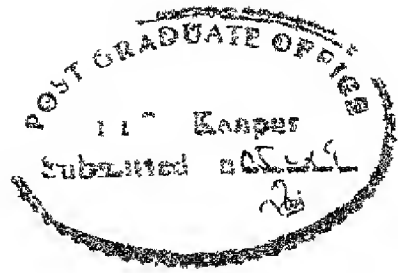## Master of Technology

by

K.Sarath Babu

to the

DEPARTMENT OF MECHANICAL ENGINEERING

INDIAN INSTITUTE OF TECHNOLOGY KANPUR

February, 1999

CERTIFICATE

It is certified that the work contained in the thesis entitled, " On the Stability of a Numerical Algorithm for the Inverse Determination of Thermal Conductivity in a 2D square Domain : a Numerical and Experimental Approach ", by K.Sarath Babu (*Roll No. 9710527*), has been carried out under our supervision and that this work has not been submitted elsewhere for a degree.

Dr.P.S.Ghoshdastidar
Associate Professor
Dept. of Mechanical Engineering
I.I.T.Kanpur

Dr.Omprakash
Assistant Professor
Dept. of Mechanical Engineering
I.I.T.Kanpur

February, 1999

Dedicated

to

my parents

Acknowledgement

Abstract

The first part of the present thesis describes an experimental technique for the inverse determination of thermal conductivity in a 2D square domain based on a finite-difference based numerical algorithm, which uses transient temperature data as the input. The algorithm is tested for a known conductivity material such as mild steel.It is found that the algorithm is highly sensitive to the measurement errors in the input data, a fact not unexpected in inverse problems which are essentially ill-posed in nature. In addition to the above mentioned experimental work, a detailed stability analysis is also performed in order to find the maximum permissible measurement error for such problems using simulated temperature profiles containing random errors. Interestingly, the study reveals that the maximum permissible measurement error is high at the early time and decreases exponentially with time. This means that early time temperature profiles should be used as input data. However, even at early times maximum allowable error in the temperature measurement is quite small which explains why the present experimental input data did not give correct conductivity value for mild steel.Future effort is needed in the direction of improving the experimental set-up so that high precision temperature measurement is possible.

-

Contents

List of Figures

List of Tables

Nomenclature

C_p specific heat of the material at constant pressure $\left(\frac{J}{kg-K}\right)$

h convective heat transfer coefficient $\left(\frac{W}{m^2-K}\right)$

k thermal conductivity of the material $\left(\frac{W}{m-K}\right)$

k_{max} Maximum conductivity value in the matrix $\left(\frac{W}{m-K}\right)$

k_{min} Minimum conductivity value in the matrix $\left(\frac{W}{m-K}\right)$

k_{th} Theoretical conductivity value $\left(\frac{W}{m-K}\right)$

k_{ouput} Conductivity value matrix obtained from inverse problem

k_{input} Conductivity value matrix given as input to get simulated temperature data

L length (m)

n number of grid points in x direction and in y direction

t time (second)

T temperature (^oC)

T_m Mean temperature value (^oC)

T_{om} Mean temperature at 0 th time (^oC)

T' Maximum noise that can be allowed theoretically (^oC)

T_o' Maximum noise at 0 th time that can be allowed theoretically (^oC)

T_o Temperature at 0 th time $\left(T_{om} + T_o'\right)$ (^oC)

$Z1, Z2, Z3, Z4.1, Z4.2$ Stability parameters

δ Error introduced in simulated temperatures (^oC)

δ_{max} Maximum allowable error in simulated temperatures to get reasonable value of 'k' by using inverse simulation (^oC)

δ_0 Maximum allowable error at 0 th time (^oC)

1

Greek Symbols

α relaxation factor

ϵ small value of temperature measurement error

ρ density of the material (kg/m^3)

Subscripts

1 at first of the two times at which input temperature is taken, also top or left boundary.

2 at last of the two times at which input temperature is taken, also bottom or right boundary.

i space index in x direction, also at t=0

j space index in y direction.

∞ ambient

Superscripts

p present time

$p + 1$ future time

$'$ first derivative

$''$ second derivative, also per unit area

Special Symbol

Δ increment

Chapter 1

Introduction and Literature Review

1.1   Introduction

The use of inverse heat conduction techniques for the determination of thermal properties such as thermal conductivity and heat capacity of solids or the estimation of surface condition such as temperature and heat flux by utilizing the transient temperature measurements taken within the medium, has numerous practical applications.

In the past decade, rapid advancement has been made in the field of materials research. This is primarily due to the demand for advanced material with low weight or the ability to withstand high temperatures required in the nuclear, electronics and aerospace industries. Precise knowledge of thermophysical properties for these materials is essential in many thermal systems. Specifically, an accurate prediction of thermal conductivity is imperative to achieve thermal control system.

The direct measurement of heat flux at the surface of a wall subjected to a fire, at the outer surface of a re-entry vehicle or at the inside surface of a combustion chamber is extremely difficult. In such situations, the inverse method of analysis, using transient temperature measurements taken within the medium can be applied for the estimation of such quantities.

An inverse problem is much more difficult to solve than the direct one. The reason for this is that it is usually ill-posed, i.e., it is very sensitive to measurement errors. An excellent discussion of difficulties encountered in inverse analysis is well documented in Beck et al (1985).

The present work involves the estimation of thermal conductivity by an inverse technique using finite-difference. Therefore, the literature review that follows concerns only the papers and texts associated with thermal conductivity measurements.

1.2 Literature Review

To date, various methods have been developed for analysis of the inverse heat conduction problem involving the estimation of thermal conductivity from measured temperatures inside the material. Beck and Arnold(1977) determined the thermal conductivity by minimizing the errors between the measured and calculated temperatures in a least squares sense. Alifanov and Mikhailov (1978) used the conjugate gradient method to solve the non-linear inverse thermal conductivity problem. Chen and Lin (1981) developed a pulse-spectrum technique (PST) based iterative numerical algorithm for remote sensing of the thermal conductivity of a non-homogeneous material for the one-dimensional (1D) case. It is found that PST does give excellent results and is more robust in solving the inverse problem of the diffusion equation than that of wave equation. Jarny et al. (1986) employed an Output Least Square Method (OLSM) to determine thermal conductivities of materials.

Tervola (1989) discussed the use of finite element method in conjunction with Davidson Fletcher-Powell method for determination of thermal conductivity of a homogeneous material from the measured temperatures at certain (finitely many) points. The work concerns the situation where the thermal conductivity is dependent on temperature. Jarny et al. (1991) employed a general optimization method using adjoint equation for solving multi-dimensional inverse heat conduction problems. Chen and co-workers (1996) employed the hybrid scheme of the Laplace Transform technique and the central difference approximation to estimate temperature dependent thermal conductivity from temperature measurements inside material at an arbitrary time. Lin and Chang (1997) proposed a numerical algorithm to estimate the thermal conductivity of a homogeneous material from boundary temperature measurements. Dowding et al. (1996) presented a laboratory method to measure the thermal properties of a carbon-carbon composite material that is characterized by an orthotropic thermal conductivity and isotropic volumetric heat capacity. Alencar Jr. et al. (1998) presented a general solution for two-dimensional boundary inverse heat conduction problem by using the conjugate gradient method of minimization together with an elliptic scheme of numerical grid generation. Simulated measurements are used to illustrate the application of the present approach to the solution of an inverse problem of practical interest.

The literature on the inverse determination of thermal conductivity from measured temperature data by finite-difference method are only a few. Lam and Yeung (1995) employed a first order finite-difference method to determine thermal conductivity in a one-dimensional (1D) heat conduction domain using Cartesian coordinates. In a subsequent paper, Yeung and Lam (1996) have successfully extended their earlier results, examining the feasibility of using a second-order finite-difference technique to determine the thermal con-

ductivity in a one dimensional (1D) heat conduction domain Recently, Ghoshdastidar and Ray (1998) presented a second-order finite-difference procedure for the inverse determination of thermal conductivity in two-dimensional (2D) square and cylindrical domains using available transient temperature data at discrete grid points. The procedure is capable of predicting constant, spatial and temperature-dependent thermal conductivities. For 2D square and cylindrical domains, the estimated thermal conductivity is verified for a constant conductivity material such as steel using numerically simulated transient temperature data.For 2D square domains, the results have also been tested against five bench mark solutions for 1D domain in which thermal conductivities are either constant or linear/non-linear function of space and temperature by forcing a 2D domain to behave like a 1D domain.The close agreement between the current results and the exact solutions confirm accuracy and effectiveness of the proposed finite-difference technique. It may be noted that the advantage of using finite-difference method is that the conductivity function can be obtained by solving the system of linear equations arising out of the discretization of the governing partial differential equation. Therefore, no prior information is required on the functional form of the thermal conductivity.

1.3   Objectives of the present study

The objectives of the present study are as follows.

1. To extend the work of Ghoshdastidar and Ray (1998) to the special case of a 2D square domain of a known constant conductivity material (mild steel) in which no heat is generated.Thus, the transient temperature data are created by obtaining numerically simulated temperature for the situation when the body is heated to a uniform temperature (T_i) and then is allowed to cool by losing heat to the ambient.

2. To develop an experimental set-up which will produce transient temperature data that will be used as the input to obtain the thermal conductivity of mild steel in a 2D square domain.

3. Since, inverse heat conduction problems are very sensitive to measurement errors, an effort is made to quantify a realistic error in conductivity by adding random errors to the simulated temperature inputs (T_{exact}).

4. To calculate conductivity using filtered T_{actual} where $T_{actual} = T_{exact}$+measurement error

5. To do a stability analysis based on 3 and 4.

3

1.4   Organization of the Thesis

The present thesis has been organized in the following manner.

▷ In Chapter 2, the finite-difference technique of Ghoshdastidar and Ray (1998) is discussed with respect to the present problem.

▷ Chapter 3, details the experimental set-up used to obtain transient temperature data required for the numerical algorithm and gives estimated conductivity values of mild steel using actual and filtered temperatures. The sources of experimental errors and possible ways to alleviate them are also mentioned.

▷ Chapter 4 presents the results of the stability analysis based on numerically simulated temperature inputs (T_{actual}) with the addition of the random measurement errors as well as that based on T_{actual} after filtering using Gram Orthogonal polynomial method described in Al-Khalidy (1998).

▷ Finally in Chapter 5, the conclusion drawn from the study and the scope for the future work are indicated.

Chapter 2

Problem Formulation

2.1 Problem Statement

Consider the problem of unsteady heat conduction in a square plate $(L \times L)$ which is initially at a temperature, T_i. Suddenly, all four sides are exposed to a cool ambient at T_∞. The problem can be assumed to be a two-dimensional one as the plate is thin so that the thermal picture in the plane normal to the Z-direction is more or less identical. The physical problem and computational domain is pictorially depicted in Fig.2.1. The simulated temperature profiles at various times have been computed using Explicit Finite-Difference scheme (Appendix 'A').

2.2 Governing Differential Equation

The governing differential equation for this case is,

$$\rho C_p \frac{\partial T}{\partial t} = k \left(\frac{\partial^2 T}{\partial x^2} + \frac{\partial^2 T}{\partial y^2} \right) + \frac{\partial k}{\partial x}\frac{\partial T}{\partial x} + \frac{\partial k}{\partial y}\frac{\partial T}{\partial y} \tag{2.1}$$

Giving the spacewise as well as time wise temperature gradients as the input to the eq. (2.1) will result in the conductivity value 'k' as output. 'k' may or may not be uniform. The next article shows the details of the finite-difference scheme.

2.3 Discretization of GDE

Equation (2.1) is discretized at each grid point (i,j) and at present time, 'p'. In this case, all the space derivatives have been discretized using suitable second order difference

5

schemes. A square grid of $\Delta x = \Delta y$ has been used. See Fig 2.2

2.3.1 Lower-Left Corner Point (1,1)

$$\rho C_p \frac{T_{i,j}^{p+1}-T_{i,j}^p}{\Delta t} = k_{i,j}\left\{\frac{-T_{i+3,j}^p+4T_{i+2,j}^p-5T_{i+1,j}^p+2T_{i,j}^p}{(\Delta x)^2} + \frac{-T_{i,j+3}^p+4T_{i,j+2}^p-5T_{i,j+1}^p+2T_{i,j}^p}{(\Delta y)^2}\right\}$$

$$+\left\{\frac{-k_{i+2,j}+4k_{i+1,j}-3k_{i,j}}{2\Delta x}\right\}\left\{\frac{-T_{i+2,j}^p+4T_{i+1,j}^p-3T_{i,j}^p}{2\Delta x}\right\}$$

$$+\left\{\frac{-k_{i,j+2}+4k_{i,j+1}-3k_{i,j}}{2\Delta y}\right\}\left\{\frac{-T_{i,j+2}^p+4T_{i,j+1}^p-3T_{i,j}^p}{2\Delta y}\right\} \tag{2.2}$$

2.3.2 Left Boundary : i=1 and j=2, n-1

$$\rho C_p \frac{T_{i,j}^{p+1}-T_{i,j}^p}{\Delta t} = k_{i,j}\left\{\frac{-T_{i+3,j}^p+4T_{i+2,j}^p-5T_{i+1,j}^p+2T_{i,j}^p}{(\Delta x)^2} + \frac{T_{i,j+1}^p-2T_{i,j}^p+T_{i,j-1}^p}{(\Delta y)^2}\right\}$$

$$+\left\{\frac{-k_{i+2,j}+4k_{i+1,j}-3k_{i,j}}{2\Delta x}\right\}\left\{\frac{-T_{i+2,j}^p+4T_{i+1,j}^p-3T_{i,j}^p}{2\Delta x}\right\}$$

$$+\left\{\frac{k_{i,j+1}-k_{i,j-1}}{2\Delta y}\right\}\left\{\frac{T_{i,j+1}^p-T_{i,j-1}^p}{2\Delta y}\right\}. \tag{2.3}$$

2.3.3 Bottom Boundary : i=2,n-1 and j=1

$$\rho C_p \frac{T_{i,j}^{p+1}-T_{i,j}^p}{\Delta t} = k_{i,j}\left\{\frac{T_{i+1,j}^p-2T_{i,j}^p+T_{i-1,j}^p}{(\Delta x)^2} + \frac{-T_{i,j+3}^p+4T_{i,j+2}^p-5T_{i,j+1}^p+2T_{i,j}^p}{(\Delta y)^2}\right\}$$

$$+\left\{\frac{k_{i+1,j}-k_{i-1,j}}{2\Delta x}\right\}\left\{\frac{T_{i+1,j}^p-T_{i-1,j}^p}{2\Delta x}\right\}$$

$$+\left\{\frac{-k_{i,j+2}+4k_{i,j+1}-3k_{i,j}}{2\Delta y}\right\}\left\{\frac{-T_{i,j+2}^p+4T_{i,j+1}^p-3T_{i,j}^p}{2\Delta y}\right\} \tag{2.4}$$

2.3.4 Lower-Right Corner Point (n, 1)

$$\rho C_p \frac{T_{i,j}^{p+1}-T_{i,j}^p}{\Delta t} = k_{i,j}\left\{\frac{-T_{i-3,j}^p+4T_{i-2,j}^p-5T_{i-1,j}^p+2T_{i,j}^p}{(\Delta x)^2} + \frac{-T_{i,j+3}^p+4T_{i,j+2}^p-5T_{i,j+1}^p+2T_{i,j}^p}{(\Delta y)^2}\right\}$$

$$+\left\{\frac{k_{i-2,j}-4k_{i-1,j}+3k_{i,j}}{2\Delta x}\right\}\left\{\frac{T_{i-2,j}^p-4T_{i-1,j}^p+3T_{i,j}^p}{2\Delta x}\right\}$$

$$+\left\{\frac{-k_{i,j+2}+4k_{i,j+1}-3k_{i,j}}{2\Delta y}\right\}\left\{\frac{-T_{i,j+2}^p+4T_{i,j+1}^p-3T_{i,j}^p}{2\Delta y}\right\} \tag{2.5}$$

2.3.5 Upper-Left Corner Point (1, n)

$$\rho C_p \frac{T_{i,j}^{p+1}-T_{i,j}^p}{\Delta t} = k_{i,j}\left\{ \frac{-T_{i+3,j}^p+4T_{i+2,j}^p-5T_{i+1,j}^p+2T_{i,j}^p}{(\Delta x)^2} + \frac{-T_{i,j-3}^p+4T_{i,j-2}^p-5T_{i,j-1}^p+2T_{i,j}^p}{(\Delta y)^2} \right\}$$

$$+ \left\{ \frac{-k_{i+2,j}+4k_{i+1,j}-3k_{i,j}}{2\Delta x} \right\}\left\{ \frac{-T_{i+2,j}^p+4T_{i+1,j}^p-3T_{i,j}^p}{2\Delta x} \right\}$$

$$+ \left\{ \frac{k_{i,j-2}-4k_{i,j-1}+3k_{i,j}}{2\Delta y} \right\}\left\{ \frac{T_{i,j-2}^p-4T_{i,j-1}^p+3T_{i,j}^p}{2\Delta y} \right\} \qquad (2.6)$$

2.3.6 Interior Grid Points : i=2,n-1 and j=2, n-1

$$\rho C_p \frac{T_{i,j}^{p+1}-T_{i,j}^p}{\Delta t} = k_{i,j}\left\{ \frac{T_{i+1,j}^p-2T_{i,j}^p+T_{i-1,j}^p}{(\Delta x)^2} + \frac{T_{i,j+1}^p-2T_{i,j}^p+T_{i,j-1}^p}{(\Delta y)^2} \right\}$$

$$+ \left\{ \frac{k_{i+1,j}-k_{i-1,j}}{2\Delta x} \right\}\left\{ \frac{T_{i+1,j}^p-T_{i-1,j}^p}{2\Delta x} \right\}$$

$$+ \left\{ \frac{k_{i,j+1}-k_{i,j-1}}{2\Delta y} \right\}\left\{ \frac{T_{i,j+1}^p-T_{i,j-1}^p}{2\Delta y} \right\} \qquad (2.7)$$

2.3.7 Right Boundary : i=n and j=2, n-1

$$\rho C_p \frac{T_{i,j}^{p+1}-T_{i,j}^p}{\Delta t} = k_{i,j}\left\{ \frac{-T_{i-3,j}^p+4T_{i-2,j}^p-5T_{i-1,j}^p+2T_{i,j}^p}{(\Delta x)^2} + \frac{T_{i,j+1}^p-2T_{i,j}^p+T_{i,j-1}^p}{(\Delta y)^2} \right\}$$

$$+ \left\{ \frac{k_{i-2,j}-4k_{i-1,j}+3k_{i,j}}{2\Delta x} \right\}\left\{ \frac{T_{i-2,j}^p-4T_{i-1,j}^p+3T_{i,j}^p}{2\Delta x} \right\}$$

$$+ \left\{ \frac{k_{i,j+1}-k_{i,j-1}}{2\Delta y} \right\}\left\{ \frac{T_{i,j+1}^p-T_{i,j-1}^p}{2\Delta y} \right\}. \qquad (2.8)$$

2.3.8 Top Boundary : i=2, n-1 and j=n

$$\rho C_p \frac{T_{i,j}^{p+1}-T_{i,j}^p}{\Delta t} = k_{i,j}\left\{ \frac{T_{i+1,j}^p-2T_{i,j}^p+T_{i-1,j}^p}{(\Delta x)^2} + \frac{-T_{i,j-3}^p+4T_{i,j-2}^p-5T_{i,j-1}^p+2T_{i,j}^p}{(\Delta y)^2} \right\}$$

$$+ \left\{ \frac{k_{i+1,j}-k_{i-1,j}}{2\Delta x} \right\}\left\{ \frac{T_{i+1,j}^p-T_{i-1,j}^p}{2\Delta x} \right\}$$

$$+ \left\{ \frac{k_{i,j-2}-4k_{i,j-1}+3k_{i,j}}{2\Delta y} \right\}\left\{ \frac{T_{i,j-2}^p-4T_{i,j-1}^p+3T_{i,j}^p}{2\Delta y} \right\} \qquad (2.9)$$

2.3.9 Upper-Right Corner Point (n, n)

$$\rho C_p \frac{T_{i,j}^{p+1}-T_{i,j}^p}{\Delta t} = k_{i,j}\left\{ \frac{-T_{i-3,j}^p+4T_{i-2,j}^p-5T_{i-1,j}^p+2T_{i,j}^p}{(\Delta x)^2} + \frac{-T_{i,j-3}^p+4T_{i,j-2}^p-5T_{i,j-1}^p+2T_{i,j}^p}{(\Delta y)^2} \right\}$$

$$+ \left\{ \frac{k_{i-2,j}-4k_{i-1,j}+3k_{i,j}}{2\Delta x} \right\}\left\{ \frac{T_{i-2,j}^p-4T_{i-1,j}^p+3T_{i,j}^p}{2\Delta x} \right\}$$

$$+ \left\{ \frac{k_{i,j-2}-4k_{i,j-1}+3k_{i,j}}{2\Delta y} \right\}\left\{ \frac{T_{i,j-2}^p-4T_{i,j-1}^p+3T_{i,j}^p}{2\Delta y} \right\} \qquad (2.10)$$

2.4 Method of Solution

Gauss-Seidel iterative method with successive under-relaxation was used to solve the set of linear simultaneous algebraic equations arising out of the discretization of eq.(2.1) at each grid point in the computational domain.The solution gives the conductivity value, 'k' at each grid point.The accuracy of the solution depends on grid spacings, time increment and the times at which the temperature profiles are taken. The values of ρ and C_p used for obtaining simulated temperatures are 7801 kg/m^3 and 473 $J/kg\ K$ respectively.It was found that a minimum of 16 grid points are required to get a reasonably accurate solution for this case since the material (Mild steel) used in this study has the conductivity of 45 $W/m.K$ which was a prior known.The double-precision arithmetic was used. The rate of convergence was quite fast The G-S iterative procedure was programmed in Fortran 77. The computations were performed using HP-9000 mainframe computer system of I.I.T. Kanpur.
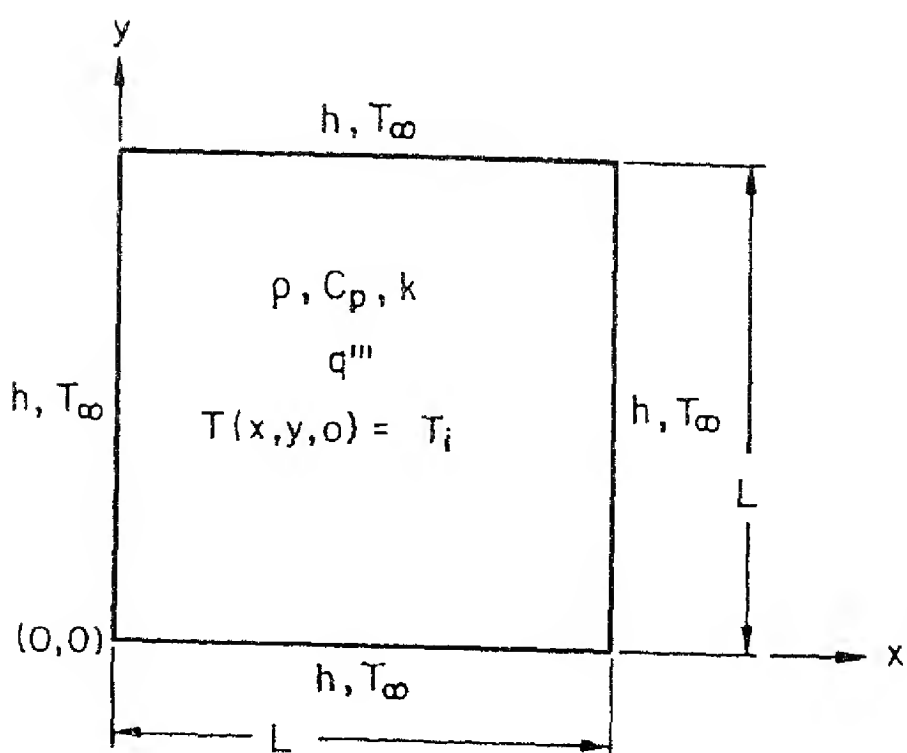
Fig.2.1 The Physical problem and the Computational domain
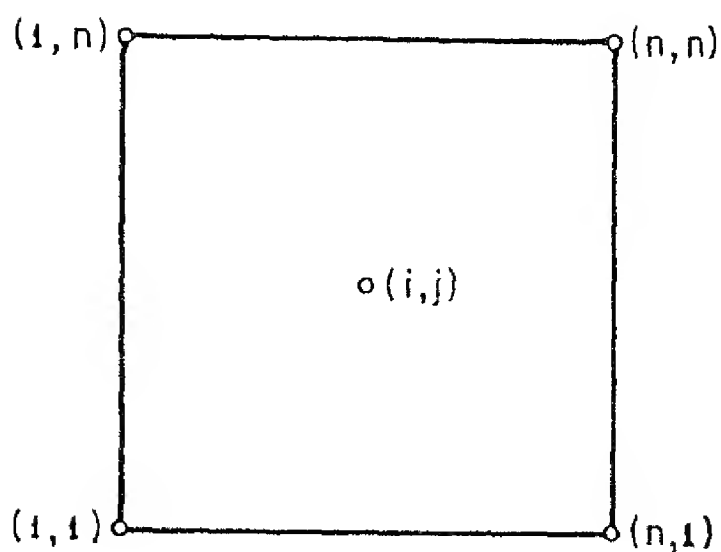
Fig.2.2 The Computational domain showing interior and corner grid points

Chapter 3

Experimental Techniques and Results

Experimental facilities and techniques used for the transient temperature measurements in a 4"×4"×0.125" specimen of mild steel to estimate its thermal conductivity are first described in this chapter.This is followed by the discussion of the results based on actually measured data and after filtering the data.The reasons for the deviation from literature value of thermal conductivity of mild steel are given at the end of this chapter.

3.1 Thermocouples

A thermocouple is a small electric device used for measuring temperatures. It consists of two wires of dissimilar metals joined at their ends, forming two junctions. If the junctions are at different temperatures, a voltage will be produced that is approximately proportional to the temperature difference, a phenomenon discovered by the German physicist Thomas Seebeck.

All temperature measurements in this study were taken with 26 SWG, Type J, insulated thermocouples, red one indicating iron and white one indicating constantan (Fig.3 1). According to Rangan et al. (1997), Type J thermocouples are made of iron as the positive thermocouple element versus constantan (57% Cr, 43% Ni) as the negative thermocouple element. They are generally recommended for use over the temperature range of -40°C to 800°C. The accuracy is usually ±2% in the range of -40 to 375°C, which the same is ±0.5%in the range of 375 to 800°C. The Type J thermocouples are inexpensive, mechanically strong but rapidly deteriorates above 600°C.In the present experiment temperature never exceeded 200°C.

3.2   Formation of Hot junction

The thermocouple hot junctions were made by flaming in the Glass blowing Workshop, I I.T. Kanpur.   Prior to that the thermocouple ends were cleaned with the help of emery paper.The quality of the junctions were determined by applying certain tension.

3.3   Calibration of Thermocouples

Temperature-measuring devices should be calibrated periodically to evaluate their performance. Such calibration can be carried out either by comparison with a standard device whose accuracy is known. This method has the advantage that the test can be performed at any desired temperature range of interest, in a bath. The attainable accuracy depends on the uniformity of the temperature distribution in the test bath and the quality of the reference standards used. The standard liquid-in-glass thermometer can be used as a reference device For tests in the range of -100 to $600^{\circ}C$, it is preferable to use an electrically-heated liquid bath. Since silicone oil baths are suitable for use as bath liquid in the temperature range of 50 to $250^{\circ}C$, all the 16 thermocouples used in this experiment were calibrated using an electrical heated silicone oil bath with a mercury-in-glass thermometer as the reference device. The calibration was done in the Refrigeration and Air-conditioning laboratory of I.I.T Kanpur.

3.4   Heater

The square specimen of Mild Steel was heated by electric 220/230 Volts AC "Heating Mantles" having energy regulator in the range of 0-100 W. The glass fibres enclosed in aluminum housing provides high thermal efficiency on the inner surface. The mantles are fitted with ON/OFF switches. The maker of the heater is Electro-Mech Instruments, Madras See Fig.3.1 for the photograph of the heater.

3.5   Preparation of the Sample and Assembly

A mild steel specimen of 4"×4"was cut from a large sheet of 0.125" thickness in the Central Workshop, I.I.T.Kanpur. The top and bottom faces were smoothed by polishing and the sides were smoothed by grinding. Next, the 16 equally spaced grid points were marked

11

on the top face. At the designated points micro holes were made so that the thermocouple hot junctions can be attached using a suitable joining technique. The distance between each thermocouple is $\frac{4}{3}$ inches. In the present case, after experimenting with various joining techniques such as use of high temperature cement, spot welding etc., it was found that brazing gave the best joint. The brazing was carried out in the TA202 Metallurgy laboratory of I.I.T. Kanpur.

After the thermocouples were brazed to the designated grid points, the strength of the joints were tested by using certain tension. the next step was to connect the cold junctions to the connectors by screwing which in turn are attached to two selector switches (Fig.3 2) each capable of handling 10 thermocouples. Finally, the positive and negative ends of the last switch were connected to the corresponding ends of the digital temperature recorder. It was ensured that the thermocouple number and the number on the switches tally.

The temperature recorder (Fig.3.2) has the range of ambient to $200°C$. Needless to say that the recorder has ambient compensation built into it. The maker of the recorder is BlueBell, Kanpur. It has an LCD display with one digit after the decimal. The accuracy of the recorder according to the supplier manual is $±0.5\%$. This was also checked against a mercury-in-glass thermometer reading of ambient as well as boiling water temperature.

3.6   General Experimental Set-up and Procedure

The Mild steel square sample supported by four tiny props was placed on an iron screen which in turn was positioned on the heater (Fig.3.3). The heating mantle was then turned on at 50W setting for 28 minutes, 70W setting for 15 minutes and 90W setting for 2 minutes till a maximum temperature of 186.0 $°C$ was shown on the digital display of the temperature recorder. The overall heating time was 45 minutes. The heating was essentially by radiation Table 3.1 at "0" time shows the temperature at the designated grid points at this point in time. Clearly, uniform temperature could not be achieved. This is in contrast with the assumption in the numerical simulation that the specimen is heated to a uniform temperature.

The next stage is the cooling of the sample. To do this the hot body was held carefully by a pair of tongs and transferred to a cooler surrounding (at a temperature of $17.2°C$). The sample was supported by four aluminum props (with sharp upper ends) as shown in Fig.3 4. During cooling, the temperature at each grid point was recorded every five minutes till 45 minutes have elapsed. The temperature history during cooling is shown in Table 3.1. The entire experiment was carried out in the Heat Transfer Laboratory. Fig.3.5 and Fig.3.6 show the actual thermocouple numbering and corresponding grid point numbering using double

subscript notation.

3.7 Results based on Actually Measured Temperatures

Table 3.2 shows the conductivity matrices calculated based on the actually measured temperatures at successive times starting from time zero. The results clearly are unsatisfactory as negative conductivity values or not a number (NaN) are not acceptable. However, this is not unexpected as it is well-known that inverse problems are highly sensitive to measurement errors in the input data. Even, 5% measurement errors can produce 50% errors in the output.

3.8 Results based on Filtered Temperatures

As mentioned in Art.3.7., the error into the results is usually greater than the error into the input data and the solution may be oscillating. Therefore, the solution may be useless when the real data are used. In this work a Gram Orthogonal Polynomial method with a moving averaging filter window is used for smoothing the noisy data. The method is based on a least square approximation. For more details, see Appendix 'B'. Table 3.3 shows the transient temperatures after 11 point filtering. Table 3.4 shows the conductivity matrices based on the filtered data. Even after filtering, there is virtually no improvement in the results pointing to a very high sensitivity of the present numerical algorithm to measurement errors The possible resons why even after filtering the results did not improve may be attributed to the fact that only timewise filtering was done. Since the present problem is 2D, spacewise filtering also should have been performed to get better results.

3.9 Sources of Experimental Errors

Since the present algorithm is very sensitive to measurement errors, it is essential that the temperature measurements are as accurate as possible. There are several reasons for not obtaining the exact temperatures. Some of them are listed below.

1. In the theoretical formulation, two-dimensional heat conduction is assumed. In actual practice, perfect two-dimensionality is very difficult to achieve.

2. There are 16 thermocouples used to measure temperatures at various grid points. These sensors are quite long and also thin. So, it produces fin effect thus decreasing the accuracy of temperature measurement.

3. The props on which the plate was heated and cooled were made of materials other than mild steel and therefore, actual temperatures were not obtained.

4. The thermocouples were brazed to the mild steel plate. The filler material for brazing is a copper-alloy (copper, zinc and tin). The filler material may also have distorted the temperature field.

5. The 16 thermocouple reading should have been taken at the same instant. In the present case, there was a time lag since it is not humanly possible to record all the temperatures at exactly the same instant.

3.10   Possible ways to avoid Experimental errors

To improve the experimental set-up, the following is suggested A PC-based transient temperature measurement should be taken with the aid of data acquisition card. Use of non-invasive technique such as thermal imaging should be looked into. Better heating and cooling arrangements are desirable. Instead of Type J, Type K (Chromel-Alumel) thermocouple can be used for higher accuracy. High precision temperature recorder should be used.
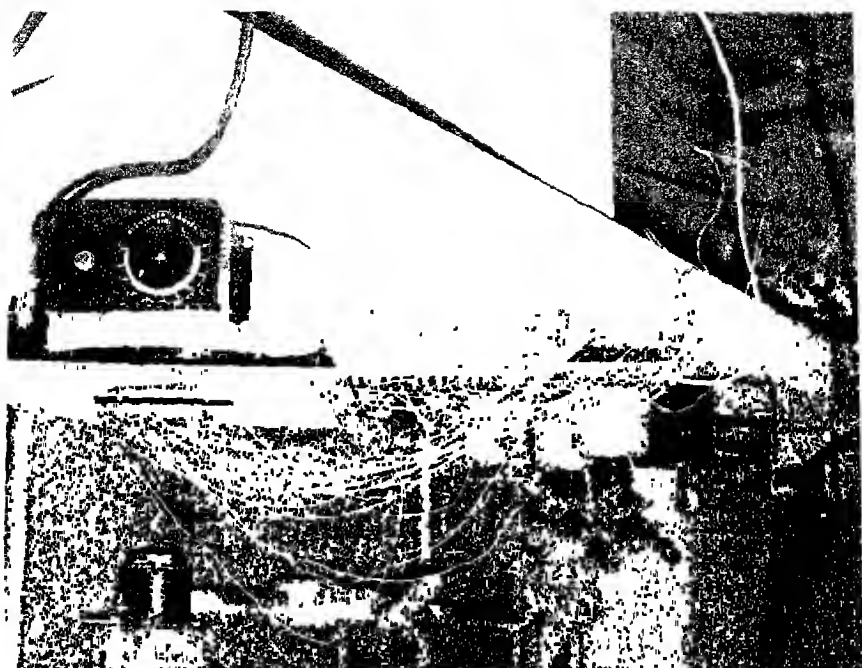
Fig 3.1 The Photograph of the heater

raph showing two selector switches and the temperature recor

Fig.3.3 The Photograph showing the heating arrangement
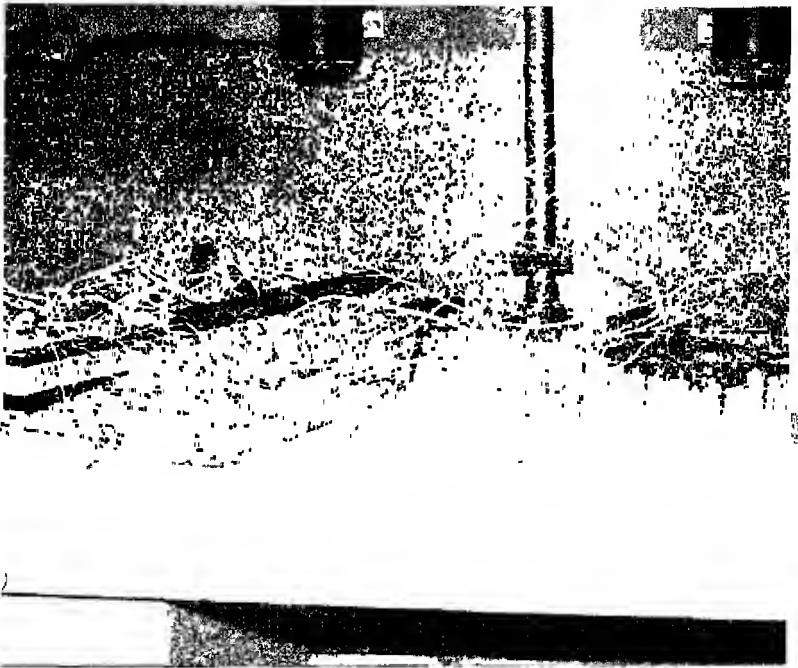
Fig 3.4 The Photograph showing the cooling arrangement
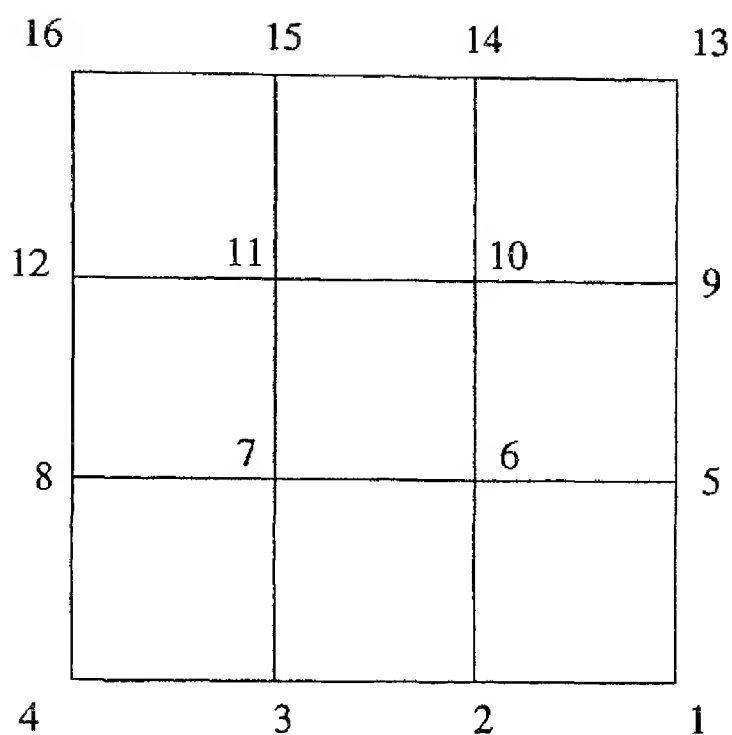
Fig.3.5 The location and numbers of the thermocouples
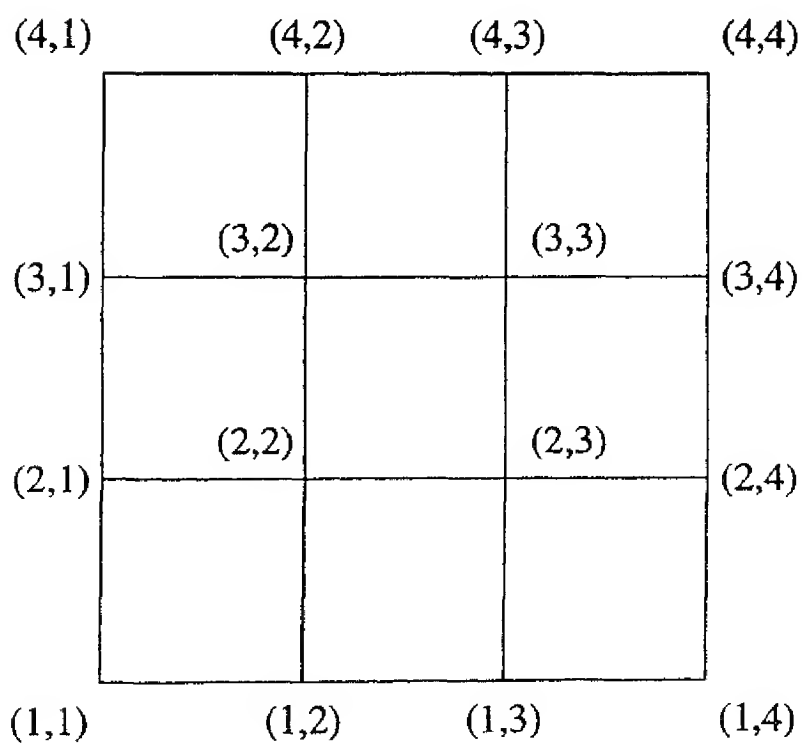
Fig.3.6 The grid point numbers using double subscript notati

I

Time (min.s)	1 (1,4)	2 (1,3)	3 (1,2)	4 (1,1)	5 (2,4)	6 (2,3)	7 (2,2)	8 (2,1)	9 (3,4)	10 (3,3)	11 (3,2)	12 (3,1)	13 (4,4)	14 (4,3)	15 (4,2)	16 (4,1)
0	184 5	172.3	162.9	171 6	186 0	167.1	163.3	164.6	175.7	152.1	178.8	156.6	170.1	171 3	177.7	163.6
5	106 6	96.1	90 8	100.0	102.9	96.5	92.1	96.2	82.0	102.6	89.0	102 7	89.7	98.0	100.4	95.5
10	61.6	56.4	54 2	59 4	61.0	57 4	55 7	56.4	52.4	61.0	55.7	60 8	56.3	58.9	59 7	57.0
15	42.6	40 3	39 3	41.3	42.2	40.9	40.2	39.9	38.5	42.5	39.6	42.4	39.3	41.3	41.9	40.5
20	32.9	31.3	30 6	32.2	32.9	32.0	31.8	31.6	31.3	33.2	31 8	33 0	31.5	32.6	32.9	32.1
25	27 9	27.0	26.6	27.6	28 0	27.4	27.4	27.3	26 9	28.2	27.4	28.1	27 4	27.9	28 1	27 7
30	25.2	24 5	24.3	24 9	25.1	25 0	24.8	25 0	24 5	25.4	24.8	25.2	24.9	25.2	25.3	24.9
35	23.7	23 4	23.2	23 5	23.7	23.6	23.5	23.6	23.4	23.9	23 6	23 8	23.6	23.8	23.7	23.7
40	22 9	22.6	22.4	22.7	22.9	22.7	22.8	22.7	22 6	23.0	22.8	22.9	22.8	22.9	22.9	22.7
45	22 3	22 2	22 1	22 3	22 4	22 3	22 3	22 3	22 1	22 4	22 4	22 5	22 3	22 5	22 4	22 4

Table 3 2 Conductivity Matrices based on Actually Measured Temperat

NaN	NaN	NaN	NaN
NaN	NaN	NaN	NaN
NaN	NaN	NaN	NaN
NaN	NaN	NaN	NaN
1.02	-2.30	54 74	-71.94
-14.77	-17.07	14.35	30.79
-32.29	-120.14	-321.57	529.78
-8.82	-15 34	-90.12	146.20
14 22	46.91	33.17	34.91
-36.78	-57.48	13.86	13.45
-172.33	-551.15	-151.34	-317.92
-273.26	-783.14	-107.23	-124.38
NaN	NaN	NaN	NaN
NaN	NaN	NaN	NaN
NaN	NaN	NaN	NaN
NaN	NaN	NaN	NaN
-1.29	-29.79	17.60	-13.19
-15.78	-12.05	14.59	12 49
-76.16	39.31	-28.77	-93.51
-.27	53.42	1.63	-9.94
50.56	-27.33	15 28	2.30
-27.91	-11.05	12.85	12.70
-822.64	49 20	-21.31	-66.69
-131.04	51.11	-3.27	-6.13
NaN	NaN	NaN	NaN
NaN	NaN	NaN	NaN
NaN	NaN	NaN	NaN
NaN	NaN	NaN	NaN
NaN	NaN	NaN	NaN
NaN	NaN	NaN	NaN
NaN	NaN	NaN	NaN
NaN	NaN	NaN	NaN
-8.67	-20 01	7.73	1.68
-11.48	-13.64	8.25	11.18
11.26	7 26	-12.85	-16.66
4.99	13.31	-5.54	8.03

(min s)	(4,1)	(4,2)	(4,3)	(4,4)	(3,1)	(3,2)	(3,3)	(3,4)	(2,1)	(2,2)	(2,3)	(2,4)	(1,1)	(1,2)	(1,3)	(1,4)
0	140.60	151.65	146.64	143.29	138.36	148.78	135.34	144.35	141.43	139.30	143.26	158.05	147.50	138.57	146.55	158.16
5	105.36	112.61	109.39	105.28	106.71	107.81	105.24	103.42	105.74	103.76	107.07	116.61	110.32	102.74	108.34	117.58
10	68.04	71.52	70.05	66.11	71.56	66.32	71.40	62.75	67.84	66.52	68.73	73.20	70.76	65.27	68.35	74.46
15	39.43	40.40	40.07	37.27	43.03	36.44	43.56	34.24	38.89	38.42	39.45	40.49	40.34	37.13	38.24	41.42
20	26.71	26.90	26.91	25.71	28.48	25.27	28.93	24.52	26.12	26.34	26.53	26.52	26.67	25.28	25.50	26.71
25	27.73	28.41	28.16	28.19	27.33	28.73	27.33	28.86	27.38	27.83	27.72	28.42	27.63	27.10	27.43	28.01
30	25.50	25.77	25.65	25.18	25.74	25.20	25.88	24.91	25.43	25.30	25.40	25.63	25.35	24.74	25.06	25.73
35	23.68	23.86	23.87	23.74	23.86	23.66	23.98	23.35	23.67	23.55	23.61	23.81	23.61	23.14	23.35	23.80
40	22.83	22.92	22.98	22.82	22.98	22.82	23.01	22.58	22.82	22.79	22.82	22.91	22.77	22.54	22.68	22.91

Table.3.4 Conductivity Matrices based on Filtered Temperatures

16 63	14 18	-5.21	5 86
17 28	25.28	-12.34	-9.31
-52 86	-40 78	-65.74	-85 07
-32 68	-17.97	24 93	-33.67
-75 51	-214 82	-51.01	5.63
92.54	125 32	-93 43	11.91
-57 20	-84.91	-96 88	-145.15
-54.23	-27.73	167.36	-130.49
NaN	NaN	NaN	NaN
NaN	NaN	NaN	NaN
NaN	NaN	NaN	NaN
NaN	NaN	NaN	NaN
-1 76	-24.63	18.13	-21 66
-7.10	-5.07	8.84	9 11
10.76	96 20	-71.00	87 35
14.79	59.91	-12.58	44.78
-.94	5.47	-1.93	7.20
1.60	4.88	1.78	-1.71
8 64	-9 49	14.80	-11.60
39	-8 41	2 33	-9.89
-1 35	-113.57	-81.92	-27.19
-18 19	-32 54	14.14	5.27
497 24	1134 41	646 55	224.18
-541.42	******	366 21	512.72
NaN	NaN	NaN	NaN
NaN	NaN	NaN	NaN
NaN	NaN	NaN	NaN
NaN	NaN	NaN	NaN
-6 76	-32.10	10 03	20.12
-11.46	-13 14	8.79	10 75
-1 43	23 38	-.15	-151 55
18 78	44.10	8 62	-39.58
-4 79	-20 81	18 90	-63.40
-8.76	-8.79	11 67	15.84
2 26	18 16	-107 44	349.24
-4 76	29.13	48 57	75 95

Chapter 4

The Effect of Noise: Simulation Studies

4.1 Introduction

The previous chapter has dealt with determination of thermal conductivity of a homogeneous plate using actual temperature measurements at discrete points and an inverse thermal conduction algorithm. It is evident that the estimated values of thermal conductivity are quite sensitive to the accuracy of the input temperature values. The errors at different points and at different times are, in general, not correlated. This can possibly lead to sharp spatial and temporal gradients in the temperature field, thereby affecting the calculated values of thermal conductivity. This results in severe inconsistencies such as prediction of negative or inaccurate conductivity values and spatially varying (in a random manner) conductivity values even when the test specimen is homogeneous. It is therefore essential to understand and quantify the effect of noise on such predictions to make such methods useful from a practical point of view. However, in an experimental set-up, it is difficult to control the level of noise as an independent parameter. An alternative approach is to simulate such problems as outlined in Figure 4.1. Initially, transient temperature data may be generated for a given problem (such as a plate of a specified material subjected to a certain temperature and then allowed to cool in atmosphere) using the direct heat-conduction formulation. Noise may be added to such data using randomly generated numbers within specified ranges. The resulting data may then be analysed using inverse calculation methods to predict the thermal conductivity of the material. The results can subsequently be compared with the conductivity value initially used for the direct problem. If the inverse method being used is based on discretization of space, such as a finite difference technique, we generally obtain a range of k values for the discrete nodal points. In this case we need to compare the goodness of the solution based on some objective measure (parameter) which considers the range of k

values obtained. In this work, we propose a number of such criteria and evaluate their relative merit. A simulation study also allows us to ascertain the utility of various filters before applying inverse methods to noisy data. In the following sections, we present the details of the simulation procedure employed and the inferences drawn.

4.2   Problem Definition: Input Parameters

We consider a homogeneous plate (4"× 4"×0.125") made of steel. The plate is initially at temperature $500^{\circ}C$ and is suddenly exposed to ambient at time t=0. The properties of mild steel are specified as:

Property	Units	Value
Thermal conductivity, k	W/mK	45.0
Density, ρ	Kg/m^3	7801.0
Specific Heat, C_p	kJ/kgK	473.0

We calculate theoretical transient temperature data at 16 grid points. The points are chosen corresponding to the locations of thermocouple attachment as described in Chapter 3.

4.3   Direct Heat-Conduction Formulation

The direct heat-conduction formulation is employed to determine the transient temperature data. We assume that there is no temperature variation in the plate-thickness direction and accordingly solve the 2D heat-conduction equation:

$$\frac{\partial T}{\partial t} = \alpha \left(\frac{\partial^2 T}{\partial x^2} + \frac{\partial^2 T}{\partial y^2} \right)$$

The boundary conditions and the method of solution using a finite difference formulation are described in Appendix 'A'. The step-size in time-increment is choosen in accordance with stability requirements (of the numerical algorithm adopted) described in Appendix 'A'.

4.4   Simulation of Noise

In inverse heat conduction problem there are a number of measured quantities such as temperature, time, senser location, and specimen thickness. We assume that the various

qu intities we accurately known except the temperature The temperature measurements we assumed to contain the major sources of error or uncertainty. Any known systematic effects due to calibration errors, presence of sensors, conduction and convection losses or others are assumed to be removed to the extent that the remaining errors may be considered to be random. These random errors can then be statistically described.

The direct problem, as described in Section 4.3 yields simulated temperature data for the inverse problem. Noise can then be added to this data in terms of random numbers within specified ranges. Thus, actual temperature T at a grid point may be given by

$$T = T_m + T'$$

where T_m is the mean (exact) temperature and T' is the noise (measurement error). If maximum noise level is specified as δ, we obtain

$$T = T_m + r.\delta$$

where r is a random number between -1 and +1.

The algorithms available for generating random numbers generally yield *pseudo random numbers*. It is therefore important to consider the statistical description of the numbers generated by any such routine.

One thousand such numbers were generated using NAG routine in the range -1 to +1. Their distribution is shown in Fig.4.2 and mean value and Standard deviation are 0.009 & 0.582 respectively.

4.5   Results and discussion

It is of interest to consider the effect of noise in simulated temperatures on inverse calculation of k value. Since we are using a finite difference algorithm, the solution is obtained in terms of spatial distribution of k values. The goodness of solution may then be quantified on the basis of prediction at a given grid-point, or in a more average sense, in terms of a parameter which takes into account the entire field solution. We adopt the latter approach and consider various alternative parameters.

4.5.1   Stability Parameters

An initial input to the direct problem is the thermal conductivity of the plate material For the 4×4 grid being used in the present case,

$$k_{input} = \begin{matrix} k_{th} & k_{th} & k_{th} & k_{th} \\ k_{th} & k_{th} & k_{th} & k_{th} \\ k_{th} & k_{th} & k_{th} & k_{th} \\ k_{th} & k_{th} & k_{th} & k_{th} \end{matrix}$$

where k_{th} is the actual (theoretical) thermal conductivity of the plate material. The corresponding distribution of k values obtained on solving the inverse problem is

$$k_{output} = \begin{matrix} k_{11} & k_{12} & k_{13} & k_{14} \\ k_{21} & k_{22} & k_{23} & k_{24} \\ k_{31} & k_{32} & k_{33} & k_{34} \\ k_{41} & k_{42} & k_{43} & k_{44} \end{matrix}$$

where k_{ij} (i=1-4. j=1-4) represents k values obtained at various grid point. The k_{output} values will range between k_{min} and k_{max}. The following parameters are now suggested for quantifying the goodness of the results.

$$Z1 = \frac{k_{min} + k_{max}}{2k_{th}}$$

$$Z2 = \frac{k_{max}}{k_{min}}$$

$$Z3 = \sqrt{\frac{\left(k_{max} - k_{th}\right)^2 + \left(k_{min} - k_{th}\right)^2}{k_{th}^2}}$$

$$Z4 : \quad Z4.1 = \frac{k_{max}}{k_{th}}, \quad Z4.2 = \frac{k_{min}}{k_{th}}$$

In the ideal case i.e. $k_{max} = k_{min} = k_{th}$, Z1, Z2 and Z4 are equal to one and Z3=0. Z1 & Z2 should be considered together to avoid misleading interpretation under special circumstances such as $k_{max} = k_{th} + \Delta k$ and $k_{min} = k_{th} - \Delta k$ Or $k_{min} = k_{max} \neq k_{th}$. In practice Z1 alone without considering Z2 gave reasonable measure of the goodness of solution.i.e. such special case was not encountered in any of the simulations.

The parameter Z3 is a more objective measure of the goodness of the solution since it considers any deviation in least-square sense. Still Z1,Z2 and Z4 are considered in this work to demonstrate that physically unacceptable (negative) values may be obtained if noise levels are high. The use of parameter Z3 fails to bring out this point.

4.5.2 Truncation and Round-off errors

The use of a numerical algorithm (both direct and inverse problems) involves truncation and rounding-off errors. Therefore, in general k_{th} and k_{output} will not be identical even if no noise were added to the simulated temperatures. A series of typical calculations and the resulting Z values for time steps n1(n1=5, t1=116.68 sec) and n2 (n2=35, t2=816.76 sec) are shown in Table 4.1. It is evident that the values of these parameters deviate from the ideal values because of truncation and rounding-off errors.The deviation is typically 3%

4.5.3 The effect of noise

Now we investigate the effect of noise on the stability parameters. Similar to Table 4 1, we go through a series of calculations except that now we add random noise to the simulated temperatures. Since the temporal gradients change with time, we repeat this simulation for various times (ranging from early to late times).

We are interested in the following :

1. What is the maximum noise level which still gives us reasonable estimate of k value (say, within $\pm 10\%$ of k_{th}) based on inverse calculations.

2. At what stage of cooling is the numerical scheme most tolerant to noise, i.e., whether early_time data is preferred over late_time data. The temporal gradients of temperature are much steeper during early time compared to late_times.

In order to study the maximum permissable noise level, the simulation was run a number of times with δ as a parameter. The value of δ ranged between 0 and 1 (insteps of 0.01). Each simulation requires temperature information at two time instants (time steps n1 and n2), which was generated using the direct formulation. Simulations were run for various pairs of n1 and n2 values to encompass a range of temporal-gradient values including early and late times.

Z values were then calculated for each simulation based on the k_{output} values obtained Typical results on the effect of noise on k_{output} values and Z parameters as a function of

26

late time and maximum noise level (actual noise at a grid point = random number in range -1 to +1 × maximum noise) are shown in Table 4.2.1 - 4.2.2, Fig. 4.3. In these es, early time refers to $n1=5$ and $n2=35$ (i.e. $t1 =116.68$ sec & $t2=816.76$ sec) and late refers to $n1 =875$ and $n2 =905$ (i.e. $t1 =20418.97$ sec & $t2 = 21119.05$ sec).Note that st row of temperature data in these tables corresponds to $\delta = 0$, i.e. no noise has been d The following trends emerge from comparision of these results.

From Fig.4.3 it is clear that the solution is close to theoretical k values up to a critical value of δ, and beyond it the solution is unstable often predicting physically unacceptable (negative) values. Z parameters can therefore be considered as parameters measuring the stability of solution This critical value can be measured in terms of acceptable deviation in Z value. So, for example, we consider the inverse prediction to be acceptable if k is within 10% of k_{th}. This gives $Z1_{(aceptable)}$ as 0.9 - 1.1 and $Z3_{(acceptable)}$ as 0.1414. Fig 4 4 shows typically the determination of critical value of δ based on Z3 parameter. This value will in general, be different at different times during the thermal history. Table 4.3 provides the critical δ values (δ_{max}) based on Z1 parameter for different times.

Inverse calculations based on early-time data yield better results than late-time data, i e., the numerical scheme can tolerate larger errors at early times. This is presumably related to steeper temporal gradients at early times.

On calculating (based on simulations) the maximum permissable error in temperature at various times during the cooling of the specimen, we find (Fig.4.5.(b)) a systematic variation of δ_{max} with t. This variation is described well in terms of an exponential decay function (Table 4.4). In (2) above, it is supposed that early time data yields better results presumably due to steeper gradients. To test this hypothesis, it was decided to plot δ_{max} w.r.t. $\frac{dT}{dt}$. The calculation of δ_{max} with $\frac{dT}{dt}$. The Values of $\frac{dT}{dt}$ at various times were calculated using noise-free data. Fig.4.6 shows this variation, based both on Z1 and Z3 parameters. It is found that a linear function (Table 4.5) describes the above data quite well, and that δ_{max} has larger value for larger $\frac{dT}{dt}$.

The simulations were also run for hypothetical materials with different values of k ($k =30, 45, 60, 75$; same ρ and C_p). In each case, the results were described well by exponential decay function (δ_{max} versus t, Fig.4.5) and linear function (δ_{max} versus $\frac{dT}{dt}$, Fig.4.7)

That such a correlation is obtained based on numerical simulation studies, merits further ttention,it is of interest to explain these results in terms of a theoretical frame work

27

In the following section, we attempt to explain these trends in terms of a lumped parameter analysis.

4.5.4   Lumped parameter analysis

Consider a lumped body, P, suddenly exposed to a surrounding media, S (Fig.4.8), at a temperature T_∞. The body P loses the heat to the media S by conduction and the media S acts as a heat sink. We assume that the boundary between P and S is such that the equivalent heat transfer coefficient in the same as thermal conductivity of P.

The governing equation for change in temperature of body P is

$$\rho C_p V \frac{dT}{dt} = kA \frac{(T_\infty - T)}{L} \qquad (4.1)$$

where L is a characteristic length scale and is of the order $\frac{V}{A}$ where V is the volume and A is the surface area of body P. For an initial temperature T_o and with both k and T_∞ independent of time, the solution of the above equation is

$$T = T_\infty - (T_\infty - T_o) \, exp \left(-\frac{kt}{\rho C_p L^2} \right) \qquad (4.2)$$

where T_o is the temperature of body P at time t=0.

In the presence of disturbance, $T = T_m + T'$ and $T_o = T_{om} + T_o'$ where subscript m refers to exact (mean) temperature and subscript (') represents the disturbance in temperature Note that the term T' represents the same physical quantity as δ. A different symbol is used here to distinguish between the notations for numerical simulation and theoretical (lumped parameter) analysis.

The above equation used in conjunction with noisy data will give reasonable estimates of k only up to a critical noise level T_{max}'; above this noise level, the numerical algorithm becomes unstable. Therefore T_{max}' may be identified as the maximum noise level which is acceptable for describing the solution in terms of equation 4.2.

Therefore we have,

$$T_m + T_{max}' = T_\infty - \left(T_\infty - \left(T_{om} + T_{o-max}' \right) \right) exp \left(-\frac{kt}{\rho C_p L^2} \right) \qquad (4.3)$$

also, for exact values of temperatures (i.e. if there were no noise),

$$T_m = T_\infty - (T_\infty - T_{om}) \exp\left(-\frac{kt}{\rho C_p L^2}\right) \qquad (4.4)$$

subtracting eq.4.4 from eq.4.3 we obtain

$$T'_{max} = T'_{0-max} \exp\left(-\frac{kt}{\rho C_p L^2}\right) \qquad (4.5)$$

The above equation implies that maximum permissable error in temperature measurement at a given time t which still gives reasonable (acceptable) values of k, decays exponentially with time. This is in agreement with Fig.4.5. Similar trend is obtained for different k_{th} values (Fig.4.5). Also, from eq.4.5,

$$\frac{T'_{max}}{T'_{o-max}} = \exp\left(-\frac{kt}{\rho C_p L^2}\right)$$

Therefore a master plot between $\frac{T'_{max}}{T'_{o-max}}$ and kt can be obtained which should be independent of k_{th} value. Fig.4.9 shows such plot on normalised axes based on the results presented in Fig.4.5.

As far as Fig. 4.10 is concerned, we can depict the theory behind it in the following manner.

From equation (4.1),

$$\frac{L^2}{\alpha} \cdot \frac{dT}{dt} = T - T_\infty \qquad (4.6)$$

where $\alpha = \frac{k}{\rho C_p}$ and $\frac{V}{A} = L$

From equation (4.2),

$$T - T_\infty = -(T_\infty - T_o) \exp(-\beta t) \qquad (4.7)$$

where $\beta = \frac{\alpha}{L^2}$

From eq. 4.6 & eq. 4.7

29

$$\frac{dT}{dt} = -\frac{\alpha}{L^2} \left(T_\infty - T_o\right) exp\left(-\beta t\right) \tag{4.8}$$

From equation (4.5) also

$$T' = T'_o exp\left(-\beta t\right) \tag{4.9}$$

Dividing equation 4.9 by equation 4.8 , we obtain

$$\frac{T'_{max}}{\frac{dT}{dt}} = -\frac{T'_o}{\left(T_\infty - T_o\right)} \cdot \frac{L^2}{\alpha}$$

or

$$T'_{max} = \left(\frac{T'_{o-max}}{k}\right) \left(\frac{L^2 \rho C_p}{\left(T_o - T_\infty\right)}\right) \cdot \frac{dT}{dt} \tag{4.10}$$

The above equation implies that T'_{max} should vary linearly with $\frac{dT}{dt}$ (since the other terms in the above equation are constant and T'_{o-max} is the maximum permissible noise at t=0). This is in good agreement with Fig.4.6-4.7. Again, the data for different k values is expected to merge if the results plotted on a normalised x-axis representing $\frac{T'_{o-max}}{k} \cdot \frac{dT}{dt}$. Although the values tend to come closer, (Fig.4.10), some variation is present presumably because all the details of a 2D problem are not captured in a lumped parameter analysis.

4.6   Effect of Filtering

In this section we consider the effect of filtering on the random errors that we imposed on the simulated temperatures.Here we are using the Gram Orthogonal Polynomial method for smoothing the noisy data,which we are getting after the addition of the random errors to the temperatures.The Gram Orthogonal Polynomial method has been described in Appendix B The main idea is to findout that whether we are getting any improved thermal conductivity values at the same level of noise after applying the filtering technique.For that we have chosen two time instants i.e for early time and for late time. At that time instants we got the simulated temperatures (direct calculation), and then added the error randomly.We then applied the filtering technique to improve the noisy data. The details are tabulated in the Table4.6. Based on these results it appears that this filtering technique is not so effective with the random errors.

Maximum Noise in temperature,δ (°C)

(a)

Maximum Noise in temperature,δ (°C)
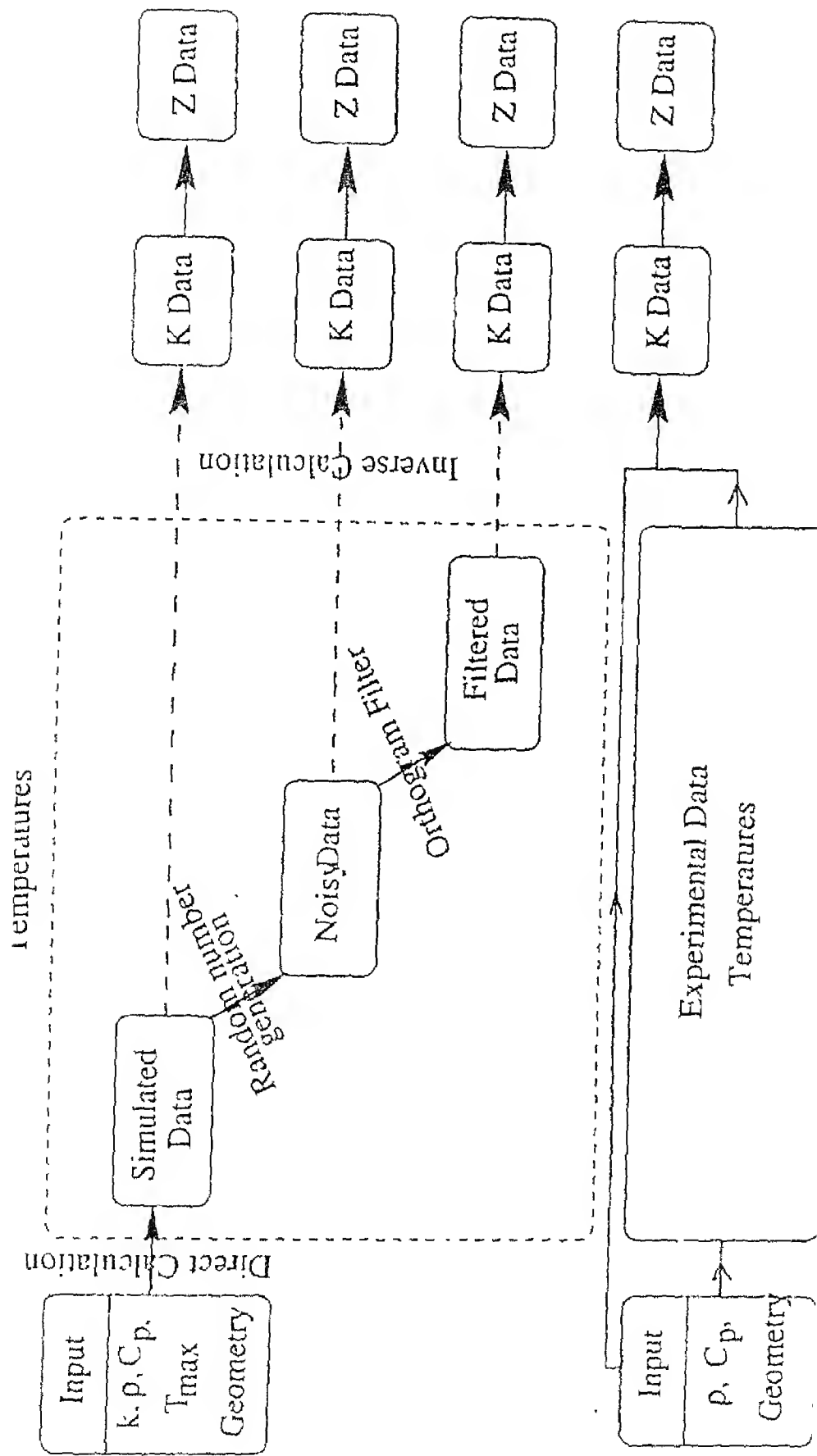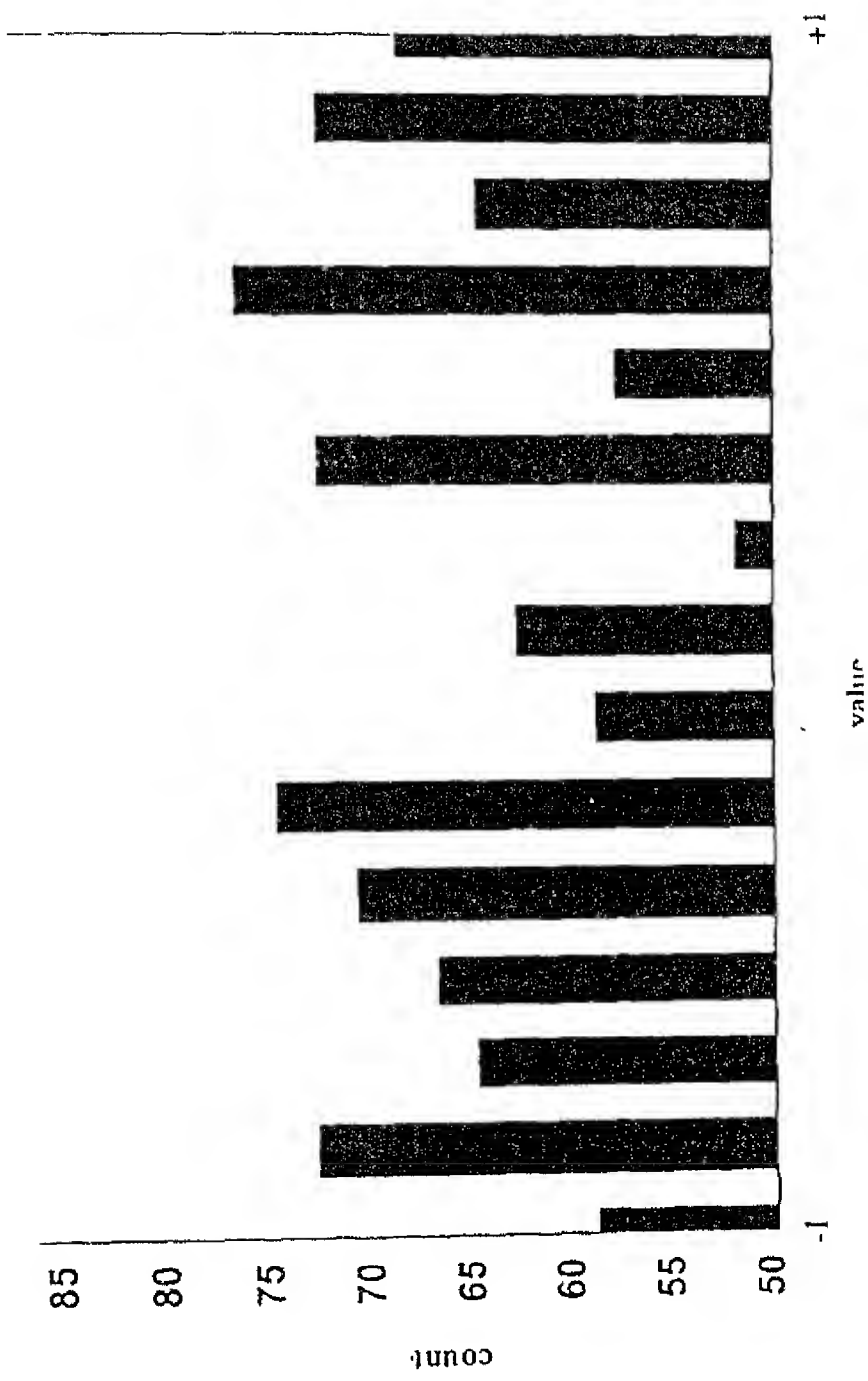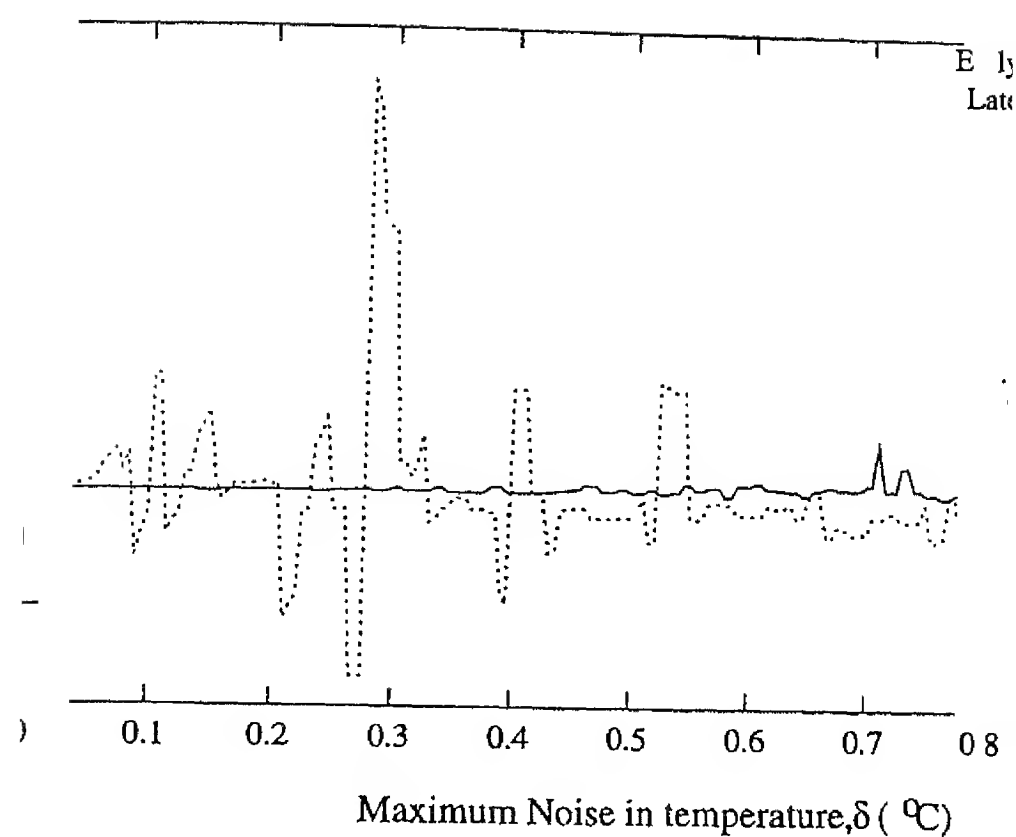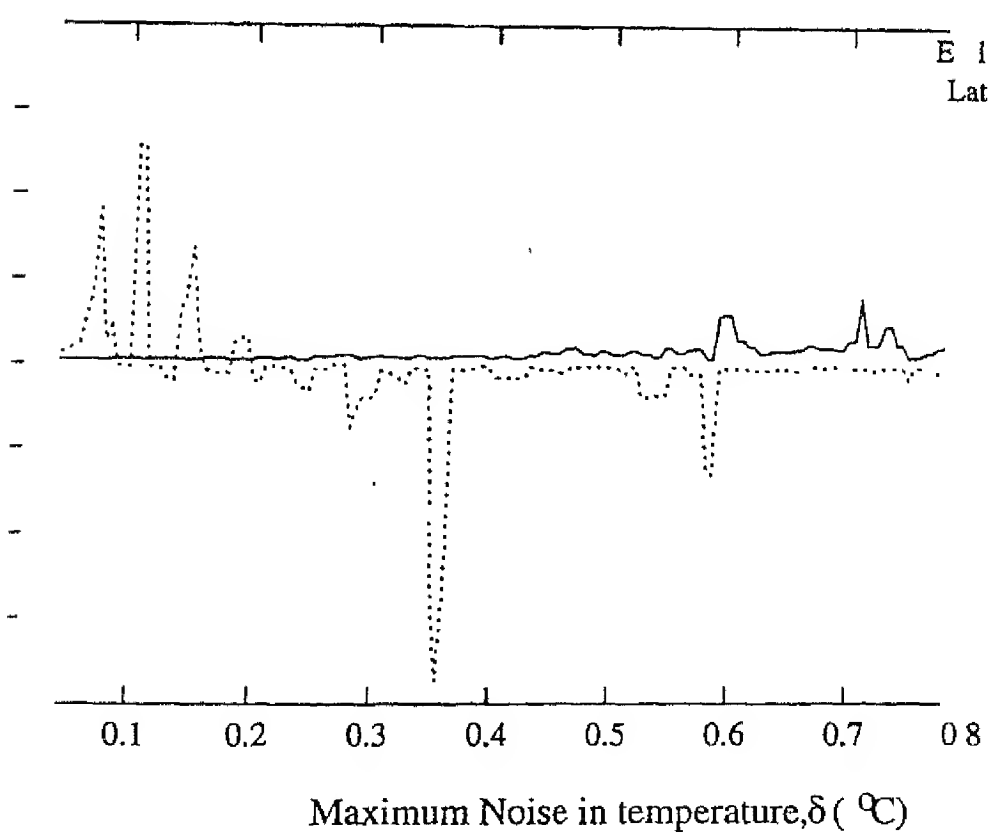
(b)

Fig 4 3 The Variation of parameters Z1 Z2,Z3and Z4 with ma
temperature (δ) at early (n1 5 n2 35) and late (n1 875 r
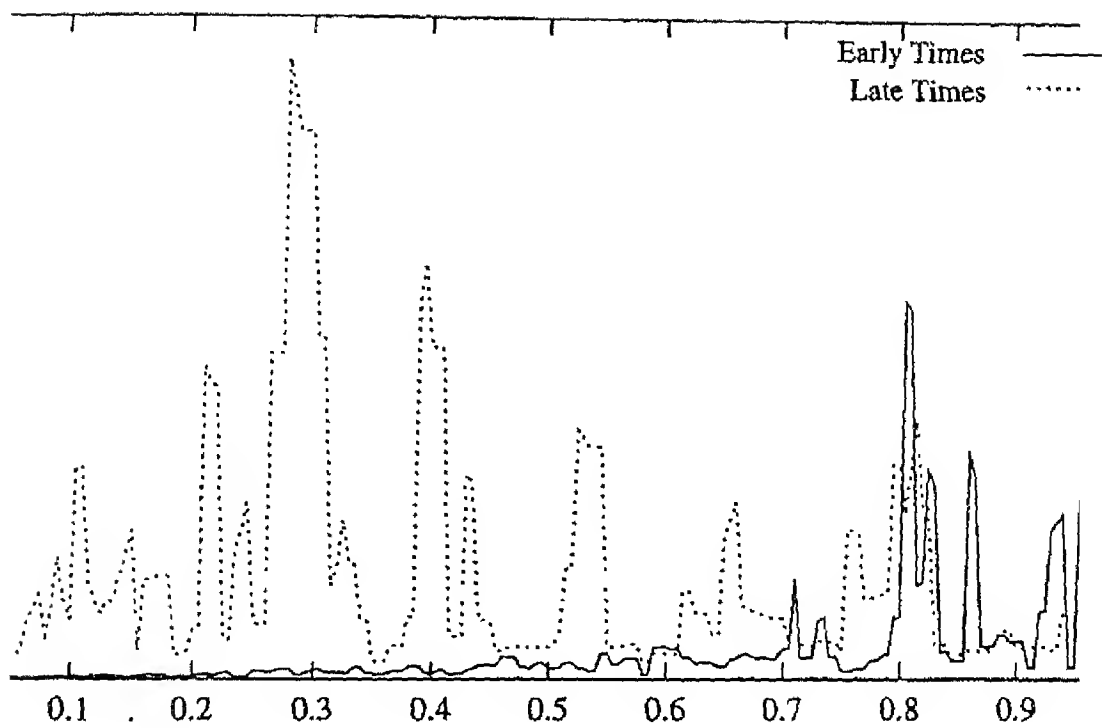
Maximum Noise in temperatures (^{o}C)

(c)

Maximum Noise in temperatures (^{o}C)

(d)

Early Time
Z3 = 0.1414
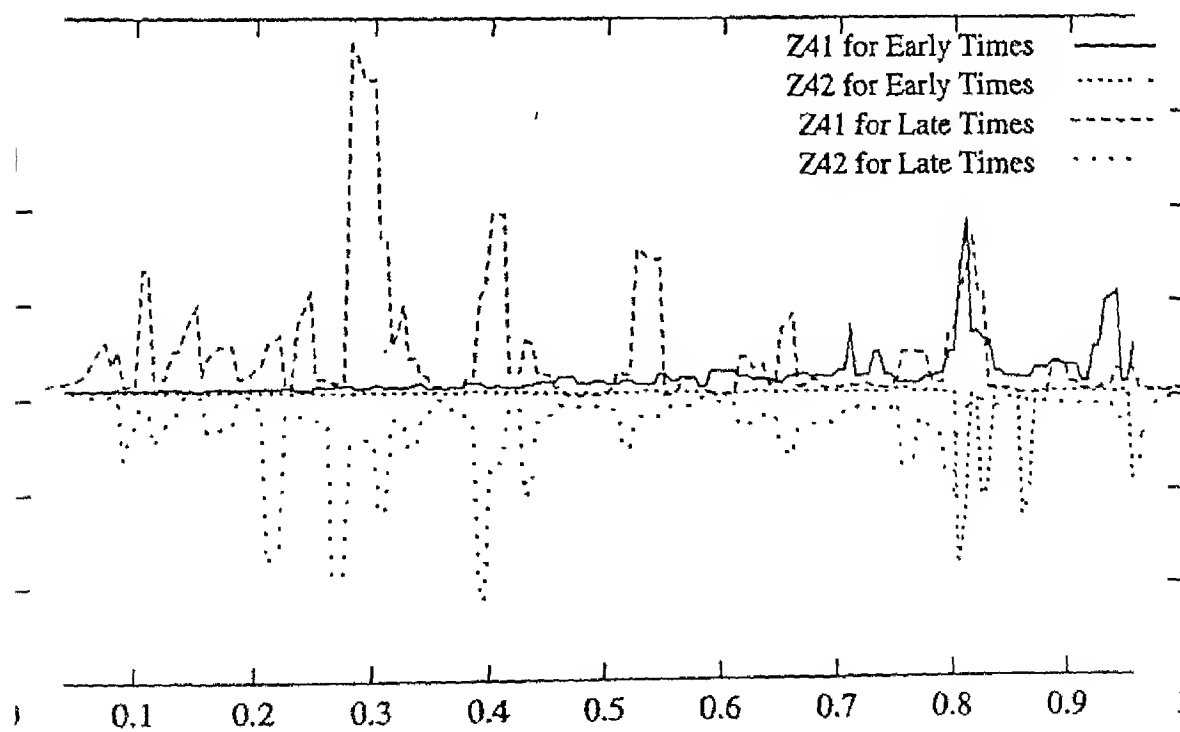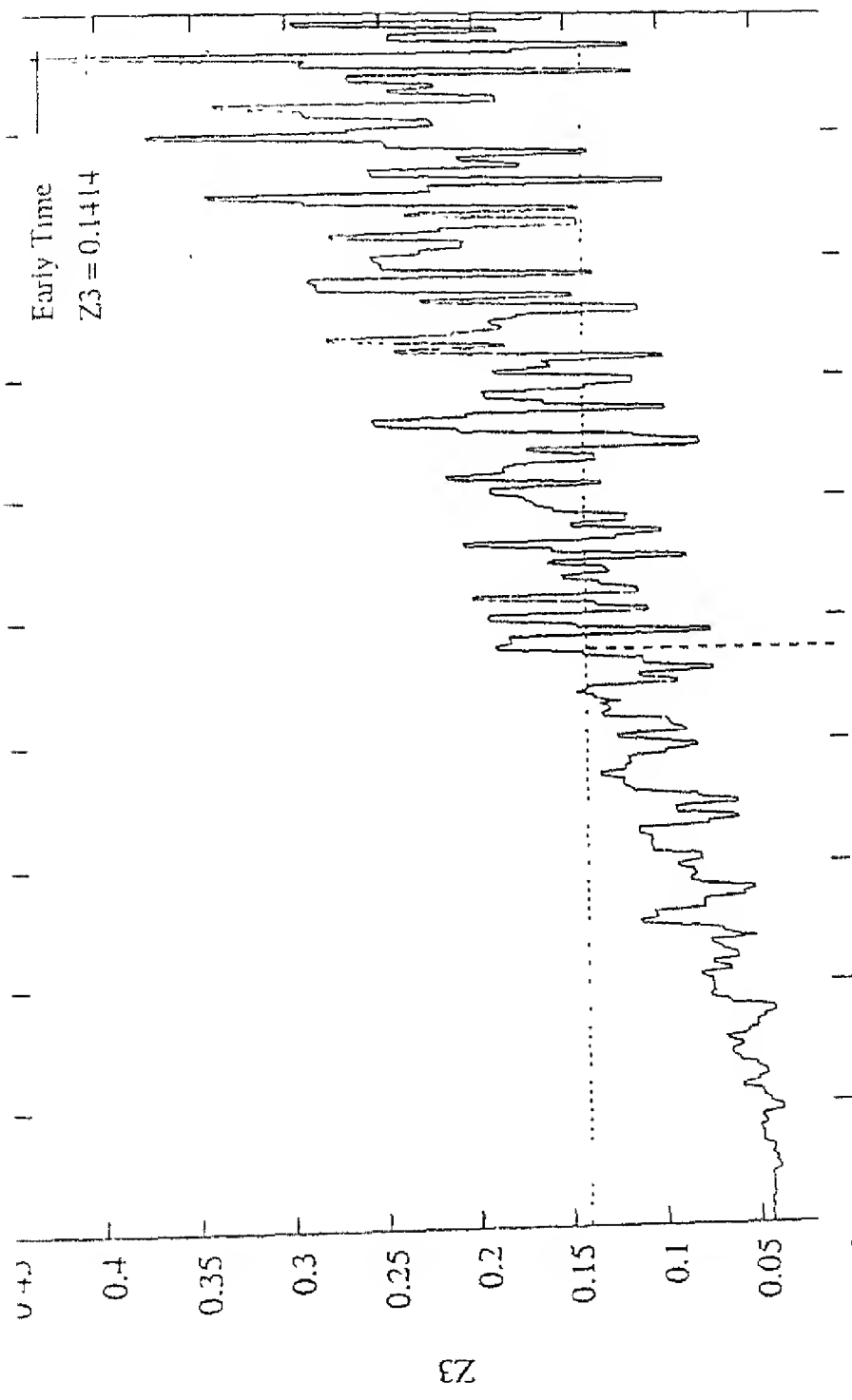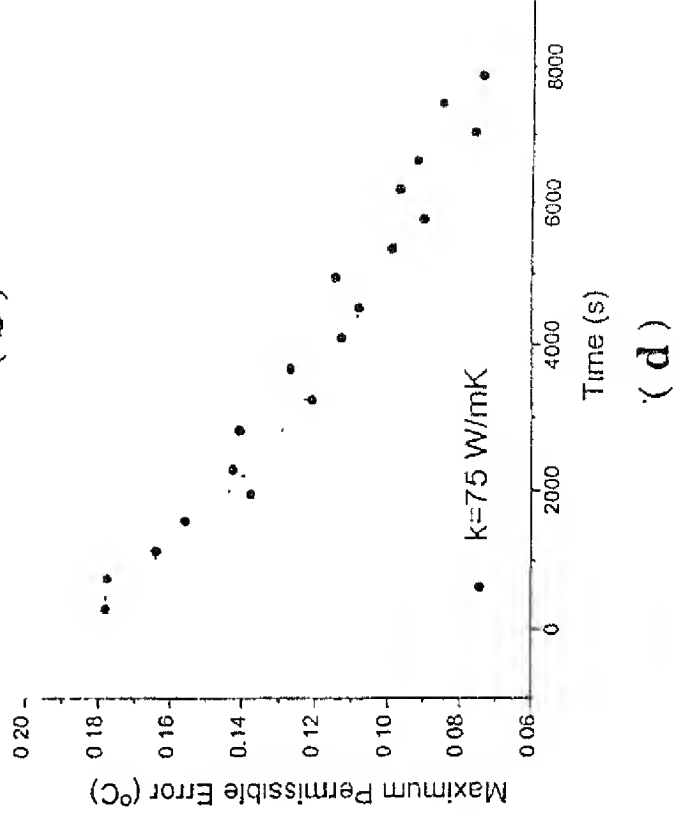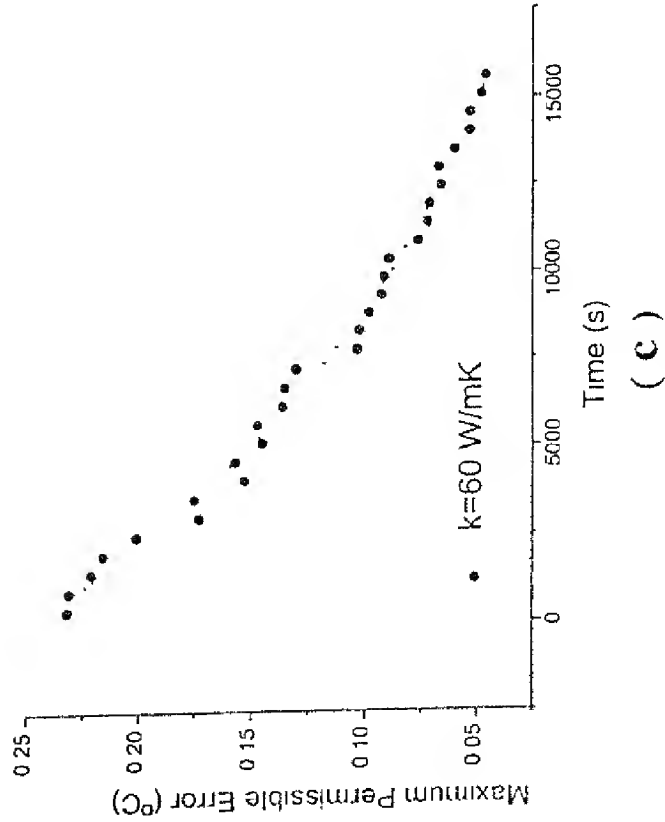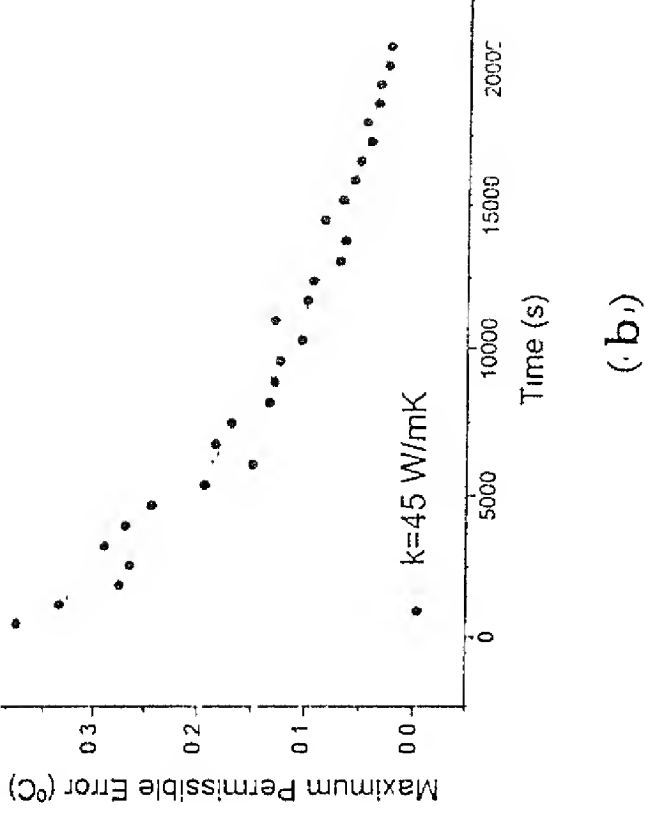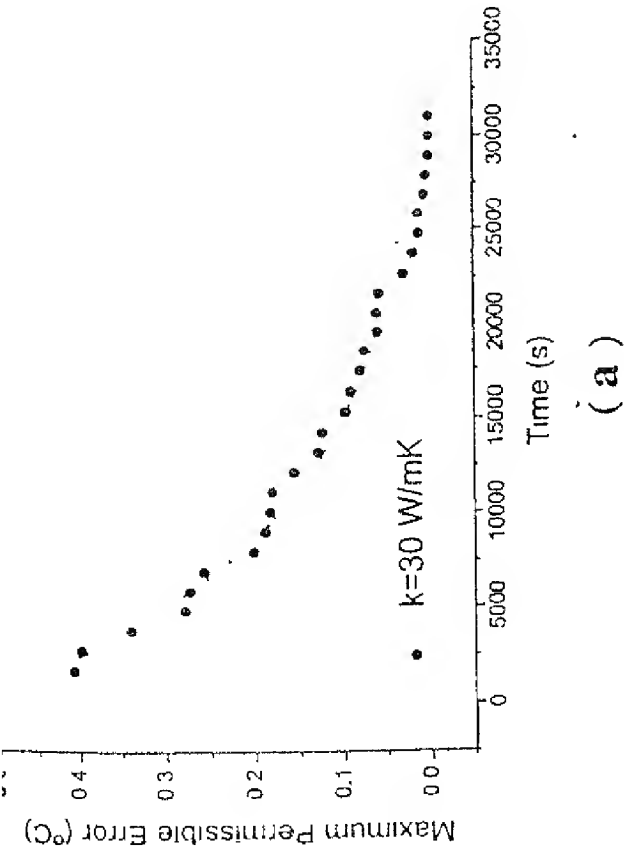
Fig.4.5 Exponential curve fitting of time Vs δ_{max} for different ' k ' values

(a) $\dfrac{dT}{dt}$

(b) $\overline{dt}$
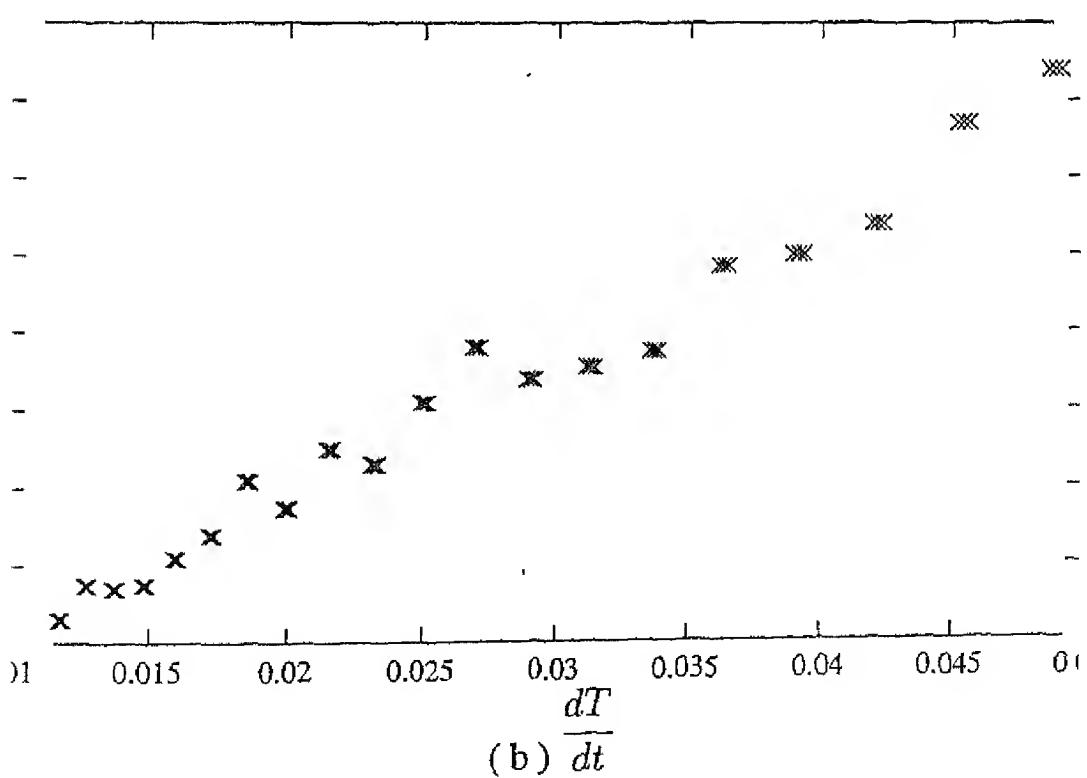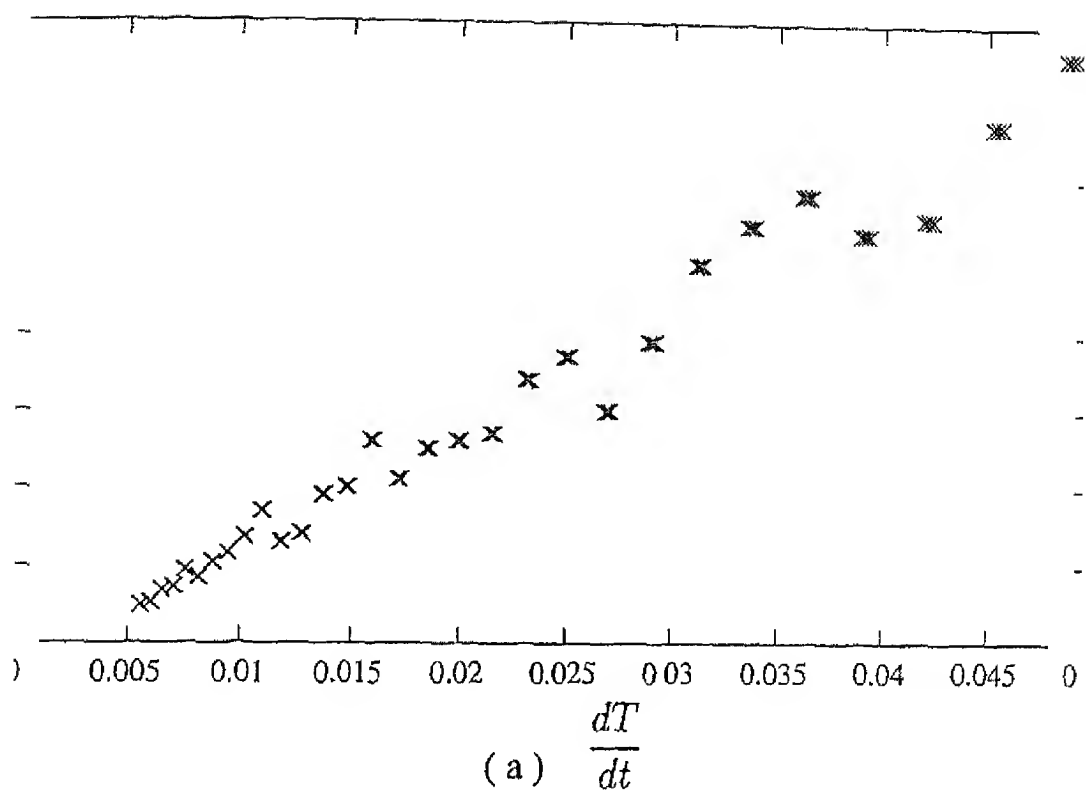
Fig.4.6 Variation of δ_{max} with $\dfrac{dT}{dt}$ based on

(a) Z1 and (b Z3 for k–45 W/m K
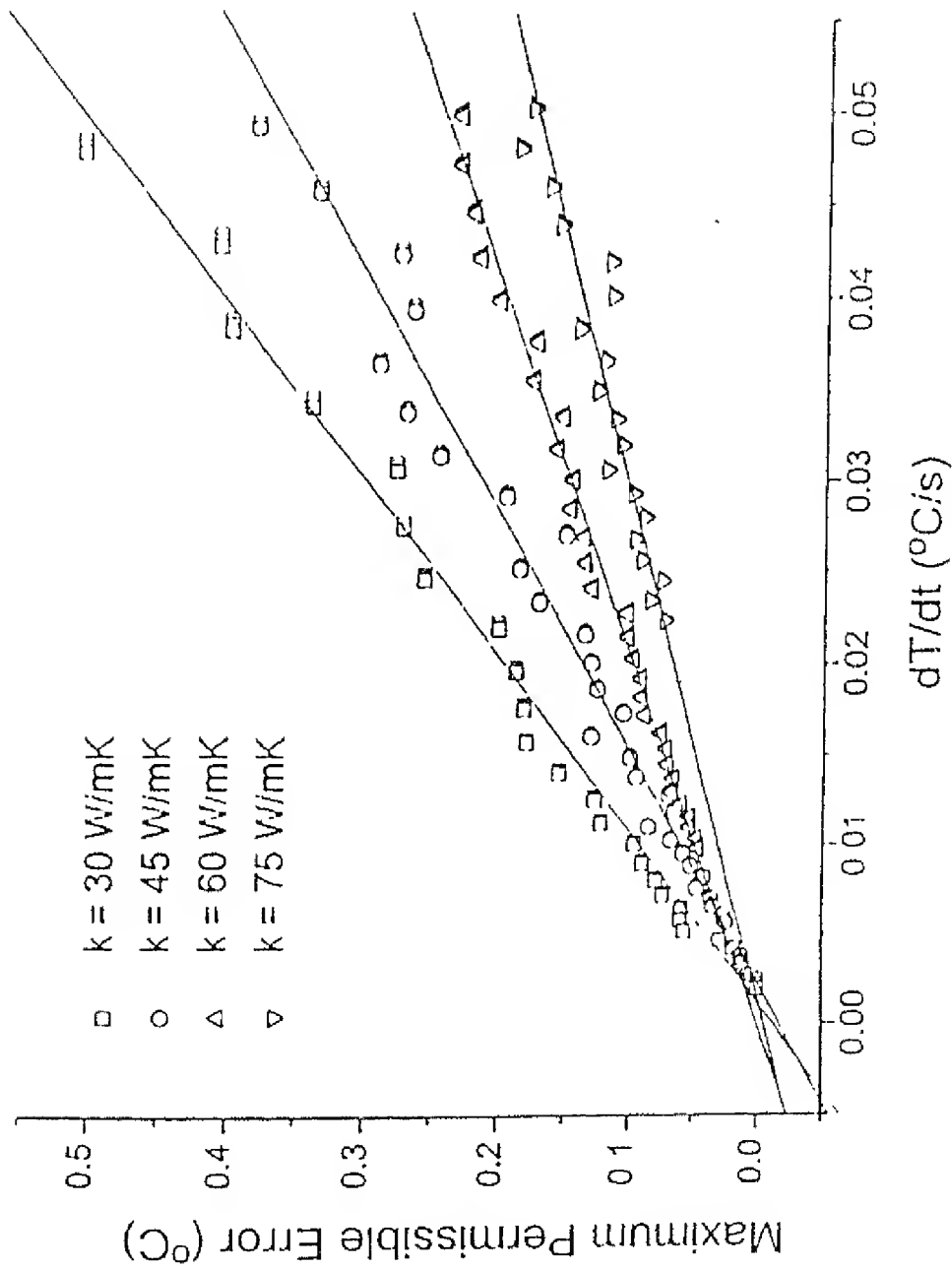
Fig 4 7 Gradient Vs δ$_{max}$ (based on Z1 values) for different k values

Fig 4.9 The graph of kt Vs δ_{max}/δ_0 for different ' k ' values

$Q\ (\delta_{max}/\delta_0)$

kt (Ws/mK)

k=30 W/mK
k=45 W/mK
k=60 W/mK
k=75 W/mK

Fig 4.10 δ_{max} Vs $\left(\dfrac{\delta_o}{k}\right)\left(\dfrac{dT}{dt}\right)$

$\delta_{max}\ (^{o}C)$

$\left(\dfrac{\delta_o}{k}\right)\left(\dfrac{dT}{dt}\right)$

k=30 W/mK
k=45 W/mK
k=60 W/mK
k=75 W/mK

P

S
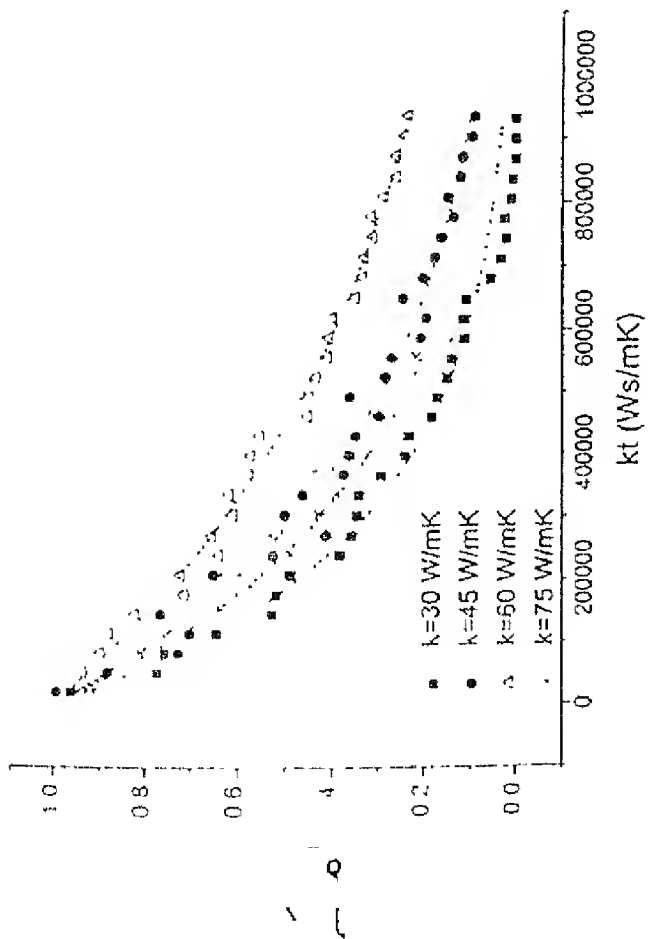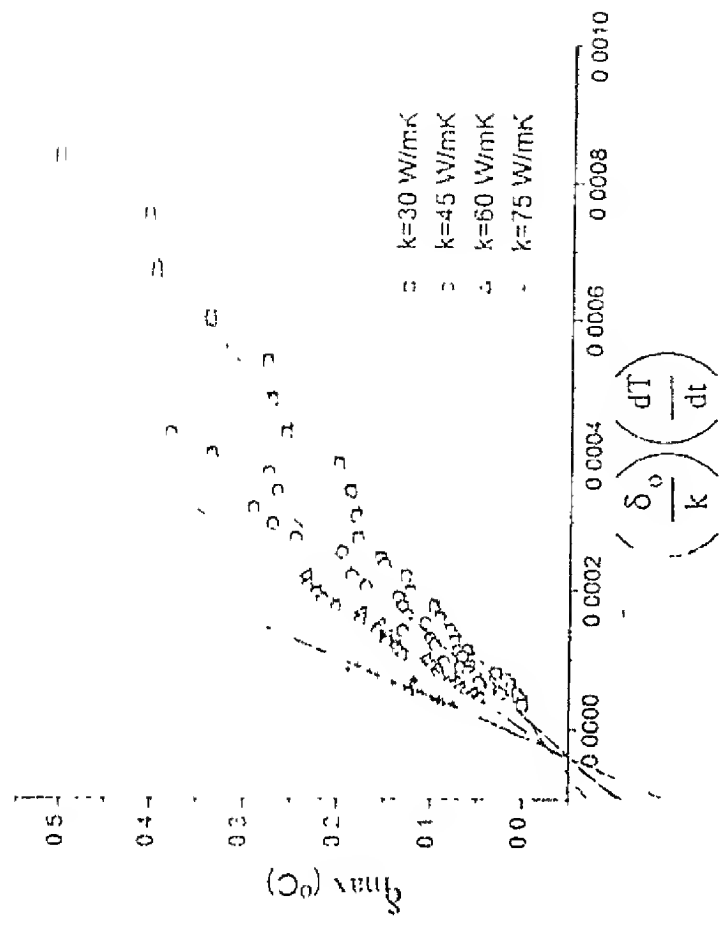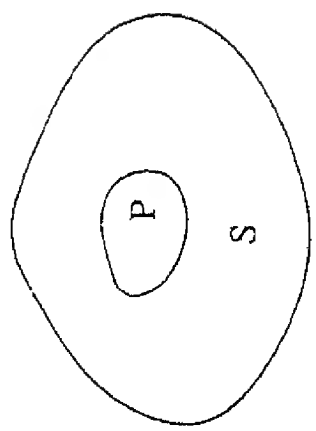
Fig.4.8 Lumped body P, exposed to the surrounding media S

Table 4.1 The effect of truncation and round-off errors in inverse problems

$$
k_{theoritcal} =
\begin{array}{cccc}
45 & 45 & 45 & 45 \\
45 & 45 & 45 & 45 \\
45 & 45 & 45 & 45 \\
45 & 45 & 45 & 45
\end{array}
$$

$Z1 = 1$

$Z2 = 1$

$Z3 = 0$

$Z4:\ Z41 = 1,\ Z42 = 1$

$\rho = 7801 kg/m^3$ $C_p = 473\ kJ/kgK$

↓ Direct Simulation

At t = 116.68 sec

490.90	493.22	493.22	490.90
493.22	495.61	495.61	493.22
493.22	495.61	495.61	493.22
490.90	493.22	493.22	490.90

At t = 816.76 sec

456.81	458.96	458.96	456.81
458.96	461.19	461.19	458.96
458.96	461.19	461.19	458.96
456.81	458.96	458.96	456.81

No noise is added

↓ Inverse Calculation

$$
k_{output} =
\begin{array}{cccc}
43.87 & 43.62 & 43.62 & 43.87 \\
43.63 & 43.39 & 43.39 & 43.63 \\
43.63 & 43.39 & 43.39 & 43.63 \\
43.87 & 43.63 & 43.63 & 43.87
\end{array}
$$

$Z1\ =\ 0.9695$

$Z2\ =\ 0.9890$

$Z3\ =\ 0.0437$

$Z4\ :\ Z41\ =\ 0.9642$

$Z42\ =\ 0.9749$

δ = 0.0

490.898	493.217	493.217	490.898	456.814	458.966	458.966	456.814	43.87	43.62	43.62	43.87
493.217	495.612	495.612	493.217	458.966	461.19	461.19	458.966	43.63	43.39	43.39	43.63
493.217	495.612	495.612	493.217	458.966	461.19	461.19	458.966	43.63	43.39	43.39	43.63
490.898	493.217	493.217	490.898	456.814	458.966	458.966	456.814	43.87	43.63	43.63	43.87

$Z1 = 0.9695$
$Z2 = 1.0110$
$Z3 = 0.0437$
$Z4.1 = 0.9749$
$Z4.2 = 0.9642$

δ = 0.20

490.969	493.359	493.179	491.091	456.722	458.888	458.825	456.787	46.64	45.35	43.9	51.55
493.132	495.551	495.575	493.139	458.784	461.167	461.298	458.834	46.62	44.56	42.6	43.54
493.364	495.537	495.542	493.253	459.144	461.176	461.084	459.1	44.38	44.55	44.63	43.44
490.92	493.019	493.15	490.849	456.947	458.918	459.059	456.67	43.04	44.01	44.71	40.7

$Z1 = 1.0250$
$Z2 = 1.2665$
$Z3 = 0.1742$
$Z4.1 = 1.1455$
$Z4.2 = 0.9044$

δ = 0.380

491.197	493.165	493.228	490.924	457.113	458.914	458.976	456.84	48.98	52.88	53.46	42.13
493.353	495.347	495.437	493.408	459.102	460.925	461.015	459.156	50.84	50.07	49.84	44.52
493.113	495.361	495.688	493.069	458.862	460.94	461.267	458.817	56.9	46.13	41.11	38.85
491.156	492.953	493.58	491.169	457.072	458.702	459.329	457.085	77.34	45.93	37.23	36.84

$Z1 = 1.2687$
$Z2 = 2.0993$
$Z3 = 0.7412$
$Z4.1 = 1.7187$
$Z4.2 = 0.8187$

δ = 0.445

491.204	493.385	492.974	491.151	457.121	459.134	458.723	457.067	46.83	50.14	45.62	78.79
493.188	495.724	495.234	492.842	458.936	461.303	460.812	458.59	35.3	40	48.05	65.28
493.446	495.988	495.297	493.258	459.194	461.566	460.876	459.006	25.79	34.04	57.81	78.29
490.658	492.803	493.653	491.046	456.574	458.551	459.402	456.962	33.22	33.86	51.04	47.31

$Z1 = 1.1620$
$Z2 = 3.0551$
$Z3 = 0.8637$
$Z4.1 = 1.7509$
$Z4.2 = 0.5731$

Table 4.2.1 The effect of noise level on Z parameters for early time steps

k & z / Temperatures / Noise	Temperatures at 16 grid points for n1=875, t1=20418.97 sec				Temperatures at 16 grid points for n1=905, t1=21119.05 sec				Thermal Conductivity values at 16 grid points				Z Parameters
$\delta=0.860$	491.524	492.864	492.678	490.618	457.441	458.612	458.426	456.534	-565.91	86.51	83.25	54.69	$Z1=-5.327$
	492.372	495.318	495.027	493.791	458.121	460.897	460.605	459.54	60.5	34.3	62.56	71.09	$Z2=-0.153$
	493.78	496.103	495.795	492.745	459.529	461.681	461.373	458.493	32.44	35.71	37.01	44.94	$Z3=13.607$
	490.171	493.574	493.539	490.7	456.088	459.323	459.287	456.616	20.77	29.97	27.34	50.65	$Z41=1.922$
													$ZA2=-12.575$
$\delta=0.960$	491.063	493.997	492.501	491.738	456.98	459.745	458.249	457.655	-204.38	-367.37	233.72	11.67	$Z1=-1.485$
	492.389	494.823	494.746	493.713	458.138	460.401	460.325	459.461	193.58	232.39	41.83	29.57	$Z2=-0.636$
	493.136	496.549	496.342	492.662	458.884	462.128	461.92	458.411	37.68	32.71	28.42	34.4	$Z3=10.077$
	490.519	493.635	493.998	490.862	456.435	459.383	459.746	456.778	2.41	-2.11	19.39	38.92	$Z41=5.193$
													$Z42=-8.164$

δ = 0.0

71.0664	71.2776	71.2796	71.0664
71.2796	71.5555	71.5555	71.2796
71.2796	71.5555	71.5555	71.2796
71.0664	71.2796	71.2796	71.0664

67.1427	67.3361	67.3361	67.1427
67.3361	67.5922	67.5922	67.3361
67.3361	67.5922	67.5922	67.3361
67.1427	67.3361	67.3361	67.1427

48.46	45.27	45.27	48.46
45.27	42.8	42.8	45.27
45.27	42.8	42.8	45.27
48.46	45.27	45.27	48.46

$Z1 = 1.014$
$Z2 = 1.132$
$Z3 = 0.031$
$Z41 = 1.076$
$Z42 = 0.95$

δ = 0.015

71.0737	71.2807	71.2914	71.0724
71.2867	71.5496	71.5693	71.2816
71.2903	71.5525	71.5483	71.2766
71.066	71.2764	71.288	71.0601

67.15	67.3373	67.3479	67.1487
67.3432	67.5864	67.606	67.3382
67.3469	67.5893	67.5851	67.3332
67.1423	67.3329	67.3446	67.1364

56.26	47.8	40.02	41.53
51.83	44.96	40.62	40.12
45.74	43.78	45.39	47.05
48.22	45.81	50.92	50.21

$Z1 = 1.049$
$Z2 = 1.405$
$Z3 = 0.274$
$Z41 = 1.250$
$Z42 = 0.889$

δ = 0.028

71.0543	71.2654	71.2711	71.0608
71.2673	71.5764	71.5346	71.2941
71.2701	71.5444	71.5676	71.3015
71.0471	71.288	71.2626	71.0866

67.1306	67.3219	67.3276	67.1371
67.3239	67.6132	67.5713	67.3507
67.3267	67.5812	67.6044	67.3581
67.1234	67.3446	67.3191	67.1629

-37.85	35.57	57.04	62.56
33.74	37.01	48.58	63.02
49.94	46.14	39.77	41.05
50.42	54.47	38.55	47.14

$Z1 = 1.075$
$Z2 = 1.867$
$Z3 = 0.472$
$Z41 = 1.400$
$Z42 = 0.749$

δ = 0.039

71.0777	71.2446	71.2654	71.043
71.2649	71.5363	71.561	71.2579
71.291	71.587	71.544	71.3095
71.0483	71.2527	71.3034	71.0983

67.154	67.3012	67.322	67.1193
67.3214	67.573	67.5978	67.3145
67.3476	67.6238	67.5808	67.3661
67.1246	67.3093	67.36	67.1746

81.83	58.13	36.88	39.49
51.81	43.25	39.15	40.77
31.73	35.55	50.41	63.29
34.99	34.8	56.33	52.96

$Z1 = 1.26$
$Z2 = 2.578$
$Z3 = 0.869$
$Z41 = 1.818$
$Z42 = 0.705$

Table 4.2.2 The effect of noise level on Z parameters for late time steps

Temperature & Z / Noise	Temperatures at 16 grid points for n1=875,t1=20418.97 sec			Temperatures at 16 grid points for n1=905,t1=21119.05 sec				Thermal Conductivity values at 16 grid points				Z Parameters
δ=0.21	70.9869	71.2336	70.9631	67.0632	67.2902	67.311	67.0394	15.84	26.48	267.58	-774.35	$Z1=-5.631$
	71.2343	71.6509	71.0782	67.2909	67.6876	67.5294	67.1348	26.64	12.87	-50.99	112.19	$Z2=-0.345$
	71.3791	71.3479	71.4306	67.4357	67.3847	67.7048	67.4872	-37.78	-53.19	16.03	18.91	$Z3=18.868$
	71.2153	71.2855	70.8618	67.2916	67.3421	67.2382	66.9381	-11.03	-26.99	24.89	7.07	$Z41=5.946$
												$Z42=-17.208$
δ=0.390	70.8047	71.0159	70.6803	66.881	67.0725	67.3974	66.7566	-863.39	97.12	10.38	-1.66	$Z1=-4.230$
	71.4782	71.2835	70.8924	67.5348	67.3202	67.801	66.949	-133.1	-92.35	6.33	21.11	$Z2=-0.559$
	71.6057	71.369	71.3441	67.6623	67.4057	67.5192	67.4007	482.7	229.03	14.89	0.64	$Z3=22.408$
	70.6971	71.0127	71.0218	66.7734	67.0692	67.1832	67.0981	358.61	164.44	135.11	16.84	$Z41=10.727$
												$Z42=-19.186$

Table 4.3 Maximum permissible values & gradient for different times based on Z1 parameter

S.No.	Time Steps		Gradient range		Maximum Permissible Error
	n1	n2			
1	5	35	0.048685	- 0.049168	0.38
2	35	65	0.045183	- 0.045638	0.335
3	65	95	0.041938	- 0.04236	0.275
4	95	125	0.038925	- 0.039317	0.265
5	125	155	0.036129	- 0.036493	0.29
6	155	185	0.033534	- 0.033872	0.27
7	185	215	0.031125	- 0.031439	0.245
8	215	245	0.02889	- 0.029181	0.195
9	245	275	0.026814	- 0.027085	0.15
10	275	305	0.024889	- 0.025139	0.185
11	305	335	0.023101	- 0.023334	0.17
12	335	365	0.021442	- 0.021658	0.135
13	365	395	0.019902	- 0.020102	0.13
14	395	425	0.018472	- 0.018658	0.125
15	425	455	0.017145	- 0.017318	0.105
16	455	485	0.015914	- 0.016074	0.13
17	485	515	0.014771	- 0.014919	0.1
18	515	545	0.01371	- 0.013848	0.095
19	545	575	0.012725	- 0.012853	0.07
20	575	605	0.011811	- 0.01193	0.065
21	605	635	0.010962	- 0.011073	0.085
22	635	665	0.010175	- 0.010277	0.068
23	665	695	0.009444	- 0.009539	0.058
24	695	725	0.008766	- 0.008854	0.052
25	725	755	0.008136	- 0.008218	0.042
26	755	785	0.007552	- 0.007628	0.047
27	785	815	0.007009	- 0.00708	0.036
28	815	845	0.006506	- 0.006571	0.034
29	845	875	0.006038	- 0.006099	0.026
30	875	905	0.005605	- 0.005661	0.024

Table 4.4 : The various terms describing the exponential equation

Equation : $y = y_0 + A\exp(-Bt)$

k	A	B	y_0	χ^2
30	0.52647	1.117e-04	0	0.0002619
45	0.39492	1.106e-04	-0.01174	0.0002699
60	0.26526	9.355e-05	-0.01618	3.747e-05
75	0.13425	2.147e-04	0.05592	0.0001322

Table 4.5 : The various terms describing the best fit linear equation

Equation : $y = A + Bx$

k	A	B	Mean	S.D.
30	-0.0124	10.4701	0.99459	0.01418
45	-0.0172	7.73875	0.98733	0.01567
60	1.015e-5	4.91502	0.99462	0.006
75	-0.00532	3.61778	0.94081	0.01099

For λ = 45 W/mK

	Temperatures at 16 grid points (for n1=5, t=116.68)				Temperatures at 16 grid points (for n2=6, t=140.02)				Thermal Conductivity values at 16 grid points			
Without Noise δ=0	490.898	493.217	493.217	490.898	489.717	492.034	492.034	489.717	45.49	45.19	45.19	45.49
	493.217	495.612	495.612	493.217	492.034	494.423	494.424	492.034	45.2	44.94	44.94	45.2
	493.217	495.612	495.612	493.217	492.034	494.424	494.424	492.034	45.19	44.93	44.93	45.19
	490.898	493.217	493.217	490.898	489.717	492.034	492.034	489.717	45.49	45.2	45.2	45.49
With Noise δ = 0.95	491.161	492.562	492.972	490.756	489.98	491.379	491.789	489.575	91.12	243.1	83.21	35.76
	493.742	494.771	494.854	493.301	492.559	493.583	493.666	492.118	27.82	8.58	58.66	65.58
	492.876	496.415	495.465	493.488	491.693	495.227	494.277	492.304	19.54	23.96	44.66	120.48
	490.231	493.126	493.71	491.615	489.051	491.942	492.527	490.435	31.22	23.18	35.33	71.35
After filtering	490.767	492.167	492.578	490.362	490.374	491.773	492.183	489.969	30.4	81.19	27.76	11.92
	493.348	494.375	494.458	492.907	492.953	493.979	494.062	492.512	9.25	2.79	19.56	21.88
	492.482	496.019	495.069	493.093	492.087	495.623	494.673	492.699	6.51	7.99	14.89	40.22
	489.838	492.731	493.316	491.222	489.444	492.337	492.921	490.828	10.42	7.74	11.78	23.8

Chapter 5

Conclusions and Scope for Future work

This work presents a finite-difference based numerical algorithm for the inverse determination of thermal conductivity in a 2D square domain using actually measured transient temperature data. It is found that for mild steel (a constant conductivity material) the algorithm is highly sensitive to the measurement errors in the input data, a fact not unexpected in inverse problems which are basically ill-posed. In addition to the experimental work, a detailed sensitivity analysis is also performed in order to find the maximum permissible measurement error (in temperature) for such problems. Interestingly, the study reveals that the maximum permissible measurement error is greater at early times and decreases exponentially with time. This means that early time temperature profiles should be used as input data. However, even at early times maximum allowable error in the temperature measurement is quite small which explains why the present experimental input data did not give correct conductivity value for mild steel.

Future effort should be directed towards improving the experimental set-up so that high precision temperature measurement is possible. A PC-based experimentation through data acquisition card is highly recommended. A non-invasive temperature measurement technique such as thermal imaging can also be looked into. A better heating and cooling arrangement is necessary.

Bibliography

[1] Alencer Jr., 1998, "A Generalized coordinates Approach for the solution of Inverse Heat conduction problems", *Proc. 11th Int. Heat Transfer Conference*, Kyongju, Korea, Vol. 7.

[2] Alifano V, O.M. and Mikhailov, V.V., 1978, "Solution of the Nonlinear Inverse Thermal conductivity problem by the Iteration method", *J.Eng.Phys.*, Vol. 35, pp. 1501-1506.

[3] Al-khalidy, Nehad, 1998, "On the Solution of Parabolic and Hyperbolic Inverse Heat conduction problems", *Int.J.Heat and Mass Transfer*, Vol. 41, pp. 3731-3740.

[4] Beck, J.V. and Arnold, K.J., 1997, *Parameter Estimation in Engineering and Science*, Wiley, New York.

[5] Beck, J.V., Blackwell B., and St.Clair, Jr., C.R., 1985 *Inverse Heat conduction*, Wiley, New York.

[6] Chen, H.T., Lin, J.Y., Wn, C.H., and Huang, C.H., 1996, "Numerical Algorithm for Estimating Temperature-dependent Thermal conductivity", *Numerical Heat Transfer, part B*, Vol. 29, pp. 509-522.

[7] Chen, Y.M., and Lin, J.R., 1981, "A Numerical Algorithm for Remote Sensing of Thermal conductivity", *Journal of Computational physics*, Vol. 43, pp. 315-326.

[8] Dowding, K.J., Beck, J.V. and Blackwell, B.F., 1996, "Estimation of Direction-Dependent Thermal properties in a carbon-carbon composite", *Int.J.Heat Mass Transfer*, Vol. 39, No. 15, pp. 3157-3164.

[9] Ghoshdastidar, P.S., and Ray, Basant, Kumar, 1998, "Inverse Determination of Thermal conductivity in Two-Dimensional Domains using Finite-Difference Technique", *Proc. 11th Int.Heat Transfer Conference*, Kyongju, Korea, Vol. 7, pp. 15-20.

[10] Janny,Y., Ozisik, M.N., and Bardon, J.P., 1991, "A General optimization Method using Adjoint Equation for solving Multidimensional Inverse Heat Conduction", *Int.J.Heat and Mass Transfer*, Vol. 34, No. 11, pp. 2911-2919.

[11] Jarny, Y., Dalaunay, D., and Bransier, J., 1986, "Identification of Nonlinear Thermal properties By an Output Least square method", *Proc. 8th International Heat Transfer Conference*, San Fransisco, Vol. 4, pp. 1811-1816.

[12] Kurpisz, K., and Nowak, A.J., 1995, *Inverse Thermal Problems*, Computational Mechanics Publications, Southampton, UK and Boston, USA.

[13] Lam, T.T., and Yeung, W.K., 1995, "Inverse Determination of Thermal conductivity for One-Dimensional problems", *Journal of Thermophysics and Heat Transfer*, Vol. 9, No. 2, pp. 335-344.

[14] Lin, Jae-yuh and Cheng, Tzai-Fu, 1997, "Numerical Estimation of Thermal conductivity from Boundary Temperature measurements", *Numerical Heat Transfer, part A*, Vol. 32, pp. 187-203.

[15] Rangan, C.S., Sarma, G.R., and Mani, V.S.V., 1997, *Instrumentation Devices & Systems*, 2nd Edition, Tata McGraw-Hill Publishing Co.Ltd., New Delhi.

[16] Tervola, Pekka, 1989, "A Method to Determine the Thermal conductivity from measured Temperature profiles", *Int.J. Heat and Mass Transfer*, Vol. 32, No. 8, pp. 1425-1430.

[17] Yeung, W.K., and Lam, T.T., 1996, "Second-order Finite Difference Approximation for Inverse Determination of Thermal conductivity", *Int.J.Heat and Mass Transfer*, Vol. 39, No. 17, pp. 3685-3693.

APPENDIX A

Determination of Simulated Temperature profile using Finite-Difference

A.1 Governing Differential Equation

The governing equation for the constant conductivty case is given by

$$\rho C_p \frac{\partial T}{\partial t} = k \left(\frac{\partial^2 T}{\partial x^2} + \frac{\partial^2 T}{\partial y^2} \right) \tag{A.1}$$

A.2 Discretization of GDE

The details of the discretization of eq.(A.1) at each grid point is described next. See Fig.2.1 for the physical problem and computational domain and Fig.2.2 for grid point numbering. The difference schemes of first and second order accuracies are given in Appendix 'C'.

A.2.1 Botom Boundary : j=1 and i=2, n-1

This surface is convecting heat to the surroundings.Therefore,

$$k \frac{\partial T}{\partial y} = h(T - T_\infty)$$

$$\Rightarrow \frac{T_{i,j+1} - T_{i,j-1}}{2\Delta y} = \frac{h}{k} \left(T_{i,j} - T_\infty \right)$$

$$\Rightarrow T_{i,j-1} = T_{i,j+1} - 2\Delta y \frac{h}{k} \left(T_{i,j} - T_\infty \right)$$

Discretizing equation (A.1), we get

$$\rho C_p \frac{T_{i,j}^{p+1} - T_{i,j}^p}{\Delta t} = k \left\{ \frac{T_{i+1,j}^p - 2T_{i,j}^p + T_{i-1,j}^p}{(\Delta x)^2} + \frac{T_{i,j+1}^p - 2T_{i,j}^p + T_{i,j+1}^p - 2\Delta y \frac{h}{k} \left(T_{i,j}^p - T_\infty \right)}{(\Delta y)^2} \right\} \tag{A.2}$$

A.2.2 Top Boundary : i=2, n-1 and j=n

This surface is convecting heat to the surroundings. Therefore,

$$-k\frac{\partial T}{\partial y} = h(T - T_\infty)$$

$$\Rightarrow \frac{T_{i,j+1}-T_{i,j-1}}{2\Delta y} = -\frac{h}{k}\left(T_{i,j} - T_\infty\right)$$

$$\Rightarrow T_{i,j+1} = T_{i,j-1} - 2\Delta y\frac{h}{k}\left(T_{i,j} - T_\infty\right)$$

Discretizing equation (A.1), we get

$$\rho C_p\frac{T_{i,j}^{p+1}-T_{i,j}^p}{\Delta t} = k\left\{\frac{T_{i+1,j}^p-2T_{i,j}^p+T_{i-1,j}^p}{(\Delta x)^2} + \frac{T_{i,j-1}^p-2T_{i,j}^p+T_{i,j-1}^p-2\Delta y\frac{h}{k}\left(T_{i,j}^p-T_\infty\right)}{(\Delta y)^2}\right\}$$

$$(A.3)$$

A.2.3 Left Boundary : i=1 and j=2, n-1

This surface is convecting heat to the surroundings. Therefore,

$$k\frac{\partial T}{\partial x} = h(T - T_\infty)$$

$$\Rightarrow \frac{T_{i+1,j}-T_{i-1,j}}{2\Delta x} = \frac{h}{k}\left(T_{i,j} - T_\infty\right)$$

$$\Rightarrow T_{i-1,j} = T_{i+1,j} - 2\Delta x\frac{h}{k}\left(T_{i,j} - T_\infty\right)$$

Discretizing equation (A.1), we get

$$\rho C_p\frac{T_{i,j}^{p+1}-T_{i,j}^p}{\Delta t} = k\left\{\frac{T_{i+1,j}^p-2T_{i,j}^p+T_{i+1,j}^p-2\Delta x\frac{h}{k}\left(T_{i,j}^p-T_\infty\right)}{(\Delta x)^2} + \frac{T_{i,j+1}^p-2T_{i,j}^p+T_{i,j-1}^p}{(\Delta y)^2}\right\}$$

$$(A.4)$$

A.2.4 Right Boundary : i=1 and j=2, n-1

This surface is convecting heat to the surroundings. Therefore,

$$-k\frac{\partial T}{\partial x} = h(T - T_\infty)$$

$$\Rightarrow \frac{T_{i+1,j}-T_{i-1,j}}{2\Delta x} = -\frac{h}{k}\left(T_{i,j} - T_\infty\right)$$

$$\Rightarrow T_{i+1,j} = T_{i-1,j} - 2\Delta x\frac{h}{k}\left(T_{i,j} - T_\infty\right)$$

Discretizing equation (A.1), we get

$$\rho C_p\frac{T_{i,j}^{p+1}-T_{i,j}^p}{\Delta t} = k\left\{\frac{T_{i-1,j}^p-2T_{i,j}^p+T_{i-1,j}^p-2\Delta x\frac{h}{k}\left(T_{i,j}^p-T_\infty\right)}{(\Delta x)^2} + \frac{T_{i,j+1}^p-2T_{i,j}^p+T_{i,j-1}^p}{(\Delta y)^2}\right\}$$

$$(A.5)$$

A.2.5 Interior Grid Points : i=2, n-1 and j=2, n-1

Discretizing equation (A.1), we get

$$\rho C_p \frac{T_{i,j}^{p+1}-T_{i,j}^p}{\Delta t} = k \left\{ \frac{T_{i+1,j}^p-2T_{i,j}^p+T_{i-1,j}^p}{(\Delta x)^2} + \frac{T_{i,j+1}^p-2T_{i,j}^p+T_{i,j-1}^p}{(\Delta y)^2} \right\}. \tag{A.6}$$

A.2.6 Lower-Left Corner Point : (1,1)

Discretizing equation (A.1), we get

$$\rho C_p \frac{T_{i,j}^{p+1}-T_{i,j}^p}{\Delta t} = k \left\{ \frac{T_{i+1,j}^p-2T_{i,j}^p+T_{i+1,j}^p-2\Delta x \frac{h}{k}\left(T_{i,j}^p-T_\infty\right)}{(\Delta x)^2} + \frac{T_{i,j+1}^p-2T_{i,j}^p+T_{i,j+1}^p-2\Delta y \frac{h}{k}\left(T_{i,j}^p-T_\infty\right)}{(\Delta y)^2} \right\} \tag{A.7}$$

A.2.7 Upper-Left Corner Point : (1, n)

Discretizing equation (A.1), we get

$$\rho C_p \frac{T_{i,j}^{p+1}-T_{i,j}^p}{\Delta t} = k \left\{ \frac{T_{i+1,j}^p-2T_{i,j}^p+T_{i+1,j}^p-2\Delta x \frac{h}{k}\left(T_{i,j}^p-T_\infty\right)}{(\Delta x)^2} + \frac{T_{i,j-1}^p-2T_{i,j}^p+T_{i,j-1}^p-2\Delta y \frac{h}{k}\left(T_{i,j}^p-T_\infty\right)}{(\Delta y)^2} \right\} \tag{A.8}$$

A.2.8 Lower-Right Corner Point : (n. 1)

Discretizing equation (A.1), we get

$$\rho C_p \frac{T_{i,j}^{p+1}-T_{i,j}^p}{\Delta t} = k \left\{ \frac{T_{i-1,j}^p-2T_{i,j}^p+T_{i-1,j}^p-2\Delta x \frac{h}{k}\left(T_{i,j}^p-T_\infty\right)}{(\Delta x)^2} + \frac{T_{i,j+1}^p-2T_{i,j}^p+T_{i,j+1}^p-2\Delta y \frac{h}{k}\left(T_{i,j}^p-T_\infty\right)}{(\Delta y)^2} \right\} \tag{A.9}$$

A.2.9 Upper-Right Corner Point : (n, n)

Discretizing equation (A.1), we get

$$\rho C_p \frac{T_{i,j}^{p+1}-T_{i,j}^p}{\Delta t} = k \left\{ \frac{T_{i-1,j}^p-2T_{i,j}^p+T_{i-1,j}^p-2\Delta x \frac{h}{k}\left(T_{i,j}^p-T_\infty\right)}{(\Delta x)^2} + \frac{T_{i,j-1}^p-2T_{i,j}^p+T_{i,j-1}^p-2\Delta y \frac{h}{k}\left(T_{i,j}^p-T_\infty\right)}{(\Delta y)^2} \right\} \tag{A.10}$$

CHECKING FOR STABILITY

The coefficient of $T_{i,j}^p$ is taken from each of the equations (A.2) - (A.10) and is it must be greater or equal tozero. In the process, we get differnet Δt's .To ensure we choose the minimum of the Δt's arising out of the stability condition.

Appendix B

Digital Smoothing Filter : Gram Orthogonal Polynomial Method

In this work a Gram orthogonal polynomial method (Al-Khalidy, 1998) with a moving averaging filter windowsis used for smoothing the noisy data. This method is based on a least square approximation. This method does not need any information about the beginning and the end of the process. This is suitable for use in on-line methods of analysis. Application of digital filtering to a series of equally spaced seven data points is shown in fig.B.1. .Digital filter replaces each data value T_k by a combination of itself and a number of adjacent nodes. Thus,

$$f_n(t_k) = \sum_{j=0}^{n} b_j p_j(k)$$

where $f(t_k)$ is the smoothed value of the measured temperature at t=k. Let L is the number of points used to the left (past temperatures) and to the right (future temperatures) of the central point at time k. The subscript 'n' refers to the total number of data points used for the smoothing process (n=5 for L=2, n=7 for L=3, etc.). The parameters in eq. (B.1) can be calculated as

$$b_j = \frac{\sum_{k=-L}^{L} T(k) p_j(k)}{\dfrac{(2L+j+1)!(2L-j)!}{(2j+1)[(2L)!]^2}}$$

$$p_j(k) = \sum_{m=0}^{j} \frac{(-1)^{m+j}(m+j)^{[2m]}(L+k)^{[m]}}{(m!)^2(2L)^{[m]}}$$

where T denotes the measured values of temperature. Thus, f(t) for each time step as the average from $T_{(t-L)}$ to $T_{(t+L)}$ is calculated. This is sometimes called moving window average. Notice that $x^{[m]} = x(x-1)(x-2)\ldots\ldots(x-m+1)$ and $m = 1, 2, 3, \ldots\ldots$

At the first steps the past temperatures can be set to be equal to the initial temperature. Similarly, at the last steps the future temperatures can be set equal to the final temperature.

The use of 7 to 11 data points is enough to obtain a good approximation. The temp
variation between two measurements should be large enough to see variation of temp
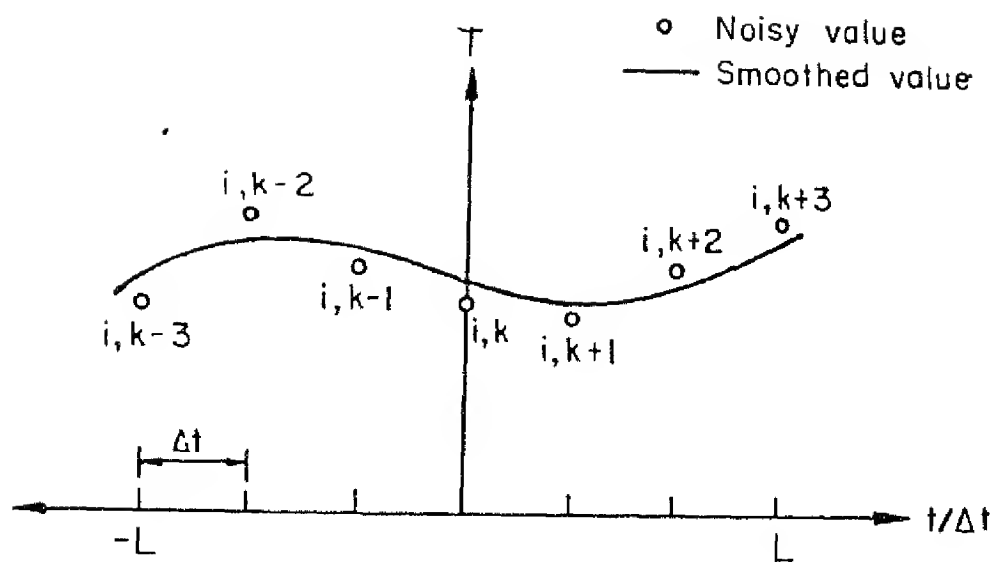and should be greater than measurement errors.

Fig. B.1 Smoothing of the measured temperatures using
seven points averaging filter.

Appendix C

Difference Schemes Of First and Second Order Accuracy

C.1 Forward difference with error $O(\Delta x)$

$$y_i' = \frac{y_{i+1} - y_i}{\Delta x} \tag{c.1}$$

$$y_i'' = \frac{y_{i+2} - 2y_{i+1} + y_i}{(\Delta x)^2} \tag{c.2}$$

C.2 Backward difference with error $O(\Delta x)$

$$y_i' = \frac{y_i - y_{i-1}}{\Delta x} \tag{c.3}$$

$$y_i'' = \frac{y_i - 2y_{i-1} + y_{i-2}}{(\Delta x)^2} \tag{c.4}$$

C.3 Forward difference with error $O(\Delta x)^2$

$$y_i' = \frac{-y_{i+2} + 4y_{i+1} - 3y_i}{2\Delta x} \tag{c.5}$$

$$y_i'' = \frac{-y_{i+3} + 4y_{i+2} - 5y_{i+1} + 2y_i}{(\Delta x)^2} \tag{c.6}$$

C.4 Backward difference with error $O(\Delta x)^2$

$$y_i' = \frac{3y_i - 4y_{i-1} + y_{i-2}}{2\Delta x} \tag{c.7}$$

$$y_i'' = \frac{2y_i - 5y_{i-1} + 4y_{i-2} - y_{i-3}}{(\Delta x)^2} \tag{c.8}$$

C.5 Central difference with error $O(\Delta x)^2$

$$y_i' = \frac{y_{i+1} - y_{i-1}}{2\Delta x} \tag{c.9}$$